Toxicology in Vitro 104 (2025) 106010

Contents lists available at ScienceDirect

Toxicology in Vitro

journal homepage: www.elsevier.com/locate/toxinvit

Transcriptomic changes and mitochondrial toxicity in response to acute and repeat dose treatment with brequinar in human liver and kidney in vitro models☆

Tamara Meijer [a,b], Bas ter Braak [c,d], Liesanne Loonstra-Wolters [c,d], Steven J. Kunnen [c], Barira Islam [e], Ilinca Suciu [f], Iain Gardner [e], Oliver Hatley [e], Richard Currie [g], Barry Hardy [h], Marcel Leist [f], Bob van de Water [c], Paul Jennings [a,b], Anja Wilmes [a,b,*]

[a] Department of Chemistry and Pharmaceutical Sciences, Vrije Universiteit Amsterdam, De Boelelaan 1108, 1081 HZ Amsterdam, the Netherlands
[b] Amsterdam Institute of Molecular and Life Sciences (AIMMS), Vrije Universiteit Amsterdam, De Boelelaan 1108, 1081 HZ Amsterdam, the Netherlands
[c] Cell Systems and Drug Safety, Leiden Academic Centre for Drug Research, Leiden University, Leiden, the Netherlands
[d] Toxys B.V., Leiden Bioscience Park, 2342 DH Oegstgeest, the Netherlands
[e] Certara – Simcyp Division, Sheffield, United Kingdom
[f] In Vitro Toxicology and Biomedicine, Department Inaugurated by the Doerenkamp-Zbinden Foundation, University of Konstanz, Universitaetsstr. 10, 78464 Konstanz, Germany
[g] Syngenta Jealott's Hill International Research Centre, Bracknell, Berkshire RG42 6EY, UK
[h] Edelweiss Connect GmbH, Technology Park Basel, Hochbergerstrasse 60C, 4057 Basel, Switzerland

ARTICLE INFO

Editor: Maxime Culot

Keywords:
Brequinar
Repeated dose toxicity
Transcriptomics
Hepatocytes
Renal proximal tubule

ABSTRACT

The potent dihydroorotate dehydrogenase (DHODH) inhibitor brequinar has been investigated as an anticancer, immunosuppressive, and antiviral pharmaceutical agent. However, its toxicity is still poorly understood. We investigated the cellular responses of primary human hepatocytes (PHH) and telomerase-immortalised human renal proximal tubular epithelial cells (RPTEC/TERT1) after a single 24-h exposure up to 100 μM brequinar. Additionally, RPTEC/TERT1 cells underwent repeated daily exposure for five consecutive days at 0.3, 3, and 20 μM. Transcriptomic analysis revealed that PHH were less sensitive to brequinar treatment than RPTEC/TERT1 cells. Upregulation of various phase I and II drug-metabolising enzymes, particularly Cytochrome P450 (CYP) 1 A and 3 A enzymes, in PHH suggests potential detoxification. Furthermore, brequinar exposure led to a significant upregulation of several stress response pathways in PHH and RPTEC/TERT1 cells, including the unfolded protein response, Nrf2, p53, and inflammatory responses. RPTEC/TERT1 cells exhibited greater sensitivity to brequinar at 0.3 μM with repeated exposure compared to a single exposure. Furthermore, brequinar could impair the mitochondrial respiration of RPTEC/TERT1 cells after 24 h. This study provides new insights into the differential responses of PHH and RPTEC/TERT1 cells in response to brequinar exposure and highlights the biological relevance of implementing repeated dosing regimens in in vitro studies.

1. Introduction

Developed in the 1980s, brequinar demonstrated promising anti-cancer effects in human cancer xenograft models (Dexter et al., 1985). Initially, brequinar was explored as a promising treatment for preventing organ graft rejection through immunosuppression (Makowka et al., 1993) and for targeting cancer (Madak et al., 2019). However, the use of brequinar in clinical settings as an anticancer agent against solid tumours was hampered by challenges in achieving effective antitumour activity without inducing unacceptable toxicity levels (Cody

☆ The peer review for this article was independently handled by the Associate Editor. The Editor-in-Chief, also the author of this article (Dr. Jennings) was not involved in the review process.

* Corresponding author at: Department of Chemistry and Pharmaceutical Sciences, Vrije Universiteit Amsterdam, De Boelelaan 1108, 1081 HZ Amsterdam, the Netherlands.

E-mail addresses: t.meijer@vu.nl (T. Meijer), s.j.kunnen@lacdr.leidenuniv.nl (S.J. Kunnen), barira.islam@certara.com (B. Islam), Barry.Hardy@edelweissconnect.com (B. Hardy), water_b@lacdr.leidenuniv.nl (B. van de Water), p.jennings@vu.nl (P. Jennings), a.wilmes@vu.nl (A. Wilmes).

https://doi.org/10.1016/j.tiv.2025.106010
Received 4 November 2024; Received in revised form 19 December 2024; Accepted 17 January 2025
Available online 1 February 2025

et al., 1993; Dodion et al., 1990; Maroun et al., 1993; Moore et al., 1993; Natale et al., 1992; Urba et al., 1992). More recently, brequinar has garnered interest for its antiviral properties (Adcock et al., 2017; Demarest et al., 2022; Qing et al., 2010) and its potential in treating acute myeloid leukemia (Sykes, 2018; Sykes et al., 2016). Despite these renewed interests, the exact mechanisms underlying brequinar-induced toxicity have yet to be fully understood.

Brequinar is a potent inhibitor of dihydroorotate dehydrogenase (DHODH), an essential enzyme involved in the de novo biosynthesis of pyrimidines, that catalyses the conversion of dihydroorotate to orotate (Chen et al., 1986; Peters et al., 1987). What distinguishes DHODH from other enzymes in this pathway is its unique localisation within the inner mitochondrial membrane in mammalian cells (Chen and Jones, 1976; Rawls et al., 2000). DHODH utilises ubiquinone as an electron acceptor, thereby functionally linking the pyrimidine biosynthesis pathway to the mitochondrial respiratory chain (Banerjee et al., 2022; Madak et al., 2019). Crystal structures of human DHODH in complex with brequinar revealed that brequinar binds to a specific tunnel that likely provides access to ubiquinone (Baumgartner et al., 2006; Liu et al., 2000). This interaction implies that brequinar inhibits DHODH activity by blocking ubiquinone access. Consequently, DHODH inhibition leads to a depletion of pyrimidine nucleotide pools, thereby impairing RNA and DNA synthesis (Chen et al., 1986; Peters et al., 1987; Schwartsmann et al., 1988).

The development of New Approach Methodologies (NAMs) as alternatives to animal testing has gained significant recognition in chemical hazard identification and risk assessment in recent years (Fischer et al., 2020; Schmeisser et al., 2023; Sewell et al., 2024). NAMs have the potential to enhance risk assessment through the utilisation of more relevant human-based models. Human in vitro systems may facilitate the elucidation of the toxicological modes of action of compounds (Bhattacharya et al., 2011). For instance, transcriptomics-based in vitro methodologies can provide comprehensive insights into chemical-induced biological perturbations on a molecular level (Wilmes et al., 2015; Wilmes et al., 2013). By assessing the differential expression of genes, cellular stress response pathways that are activated in response to toxin exposure can be identified, thereby aiding in the delineation of the mechanisms underlying toxicity (Jennings et al., 2013). Several transcriptomic studies have demonstrated the value of integrating cellular stress response pathway analysis for toxicity prediction and assessment in various human in vitro models (Capinha et al., 2023; Fernandes et al., 2020; Jennings et al., 2023; Krauskopf et al., 2022; Murphy et al., 2024; Nunes et al., 2022; ter Braak et al., 2021). These studies illustrate that, by applying a transcriptomics-based approach, it is possible to effectively identify perturbed cellular pathways and visualise transcriptomic fingerprints, which may aid in the prediction and classification of compound- and tissue-specific toxicity. Nevertheless, the majority of in vitro studies primarily focus on single exposure scenarios and often neglect repeat dose testing. While single exposure testing is valuable for identifying acute toxic effects, it may not accurately reflect real-life exposure scenarios where repeated exposure to drugs is more common. This is of particular concern for compounds that might be accumulated in the cells after repeated exposures.

In the present study, we aimed to investigate the mechanisms of toxicity induced by the DHODH inhibitor brequinar in primary human hepatocytes (PHH) and telomerase-immortalised human renal proximal tubular epithelial cells (RPTEC/TERT1), representing in vitro models of the liver and kidney, respectively. Given their crucial roles in drug metabolism and elimination, the liver and kidney are frequent target organs of toxicity and are therefore particularly important in drug safety assessment and prediction. We assessed the cellular responses of PHH and RPTEC/TERT1 cells following a single exposure (24 h) to brequinar. Additionally, we examined the transcriptomic profile of RPTEC/TERT1 cells after the repeated administration (every 24 h for five consecutive days) of brequinar.

2. Materials and methods

2.1. Cell culture

LIVERPOOL cryoplateable PHH from 10 pooled donors (BioIVT, X008001) were stored at −150 °C until use. Cells were thawed by holding the vial in a 37 °C water bath for 2 min and subsequently transferred into 50 mL of pre-warmed thawing medium (OptiThaw Hepatocyte Kit, XenoTech, K8000). After centrifugation for 10 min at 100 ×*g* at room temperature, cells were resuspended in pre-warmed seeding medium (500 mL INVITROGRO CP Medium, BioIVT, Z990003, supplemented with 5.5 mL TORPEDO Antibiotic Mix, BioIVT, Z99000). The live cells were counted to determine the post-thaw viability using the Trypan Blue exclusion method. Next, cells were plated at a seeding density of 70,000 cells/well in Corning™ BioCoat™ Collagen I 96-well plates and placed in a humidified 5 % CO_2 incubator at 37 °C. The seeding medium was replaced with maintenance medium (500 mL INVITROGRO HI Medium, BioIVT, Z990012, supplemented with 5.5 mL TORPEDO Antibiotic Mix) 6 h after plating. One day (24 h) after plating, the cells were exposed to brequinar.

RPTEC/TERT1 cells (Wieser et al., 2008), obtained from Evercyte GmbH (Vienna, Austria), were routinely cultured in a 1:1 mixture of Dulbecco's modified Eagle Medium (DMEM) (Gibco, 11966–025) and Ham's F-12 nutrient mix (Gibco, 21765–029) supplemented with 2 mM glutamax (Gibco, 35050–038), 5 μg/mL insulin, 5 μg/mL transferrin, 5 ng/mL sodium selenite (ITS) (Sigma-Aldrich, I1884), 10 ng/mL epidermal growth factor (EGF) (Sigma-Aldrich, E9644), 36 ng/mL hydrocortisone (Sigma-Aldrich, H0135), 100 U/mL penicillin, 100 μg/mL streptomycin (Pen-Strep) (Sigma-Aldrich, P4333), and 0.5 % fetal bovine serum (FBS) (Gibco, 10270–106), at 36.5 °C in a humidified 5 % CO_2 incubator, as previously described (Capinha et al., 2023). For experiments, cells were passaged into 96-well plates (Greiner Bio-One). For the MitoStress assay, the dedicated Seahorse XF96 V3 PS Cell Culture Microplates (Agilent, 101085–004) were used instead. Cells were plated at a seeding density of 15,000 cells/well in 96-well plates and 25,000 cells/well in Seahorse plates. Before starting compound exposure, cells were cultured for a minimum of 7 days after reaching confluency. Importantly, cells in the Seahorse Microplates were cultured for a longer period of time to allow differentiation (approximately 14 days after reaching confluency), during which dome formation was carefully monitored. RPTEC/TERT1 cells were used between passages 77 and 94.

2.2. Compound preparation and dosing schedules

Brequinar (CAS number 96187–53-0) was obtained from Syngenta (Basel, Switzerland) and prepared as a 0.1 M stock solution in dimethyl sulfoxide (DMSO) (Sigma-Aldrich, D8418). Sodium arsenite (Sigma-Aldrich, S7400) was dissolved in nanopure water to a stock concentration of 0.01 M and tunicamycin (Tocris Bioscience, 3516) in DMSO to 0.05 M. Sodium arsenite was taken along as positive control for the activation of the Nuclear Factor Erythroid 2 Like 2 (*NFE2L2*, also called Nrf2) pathway (Fig. S1). While sodium arsenite is a relatively strong inducer of the Nrf2 oxidative stress response, it should be noted that it is also inducing other stress response pathways, e.g. the metal stress response (Jennings et al., 2023). Tunicamycin was included as positive control for the induction of the unfolded protein response (UPR) (Fig. S1). All stock solutions were stored at −20 °C until use. For experiments, treatment solutions were freshly prepared by directly performing serial dilutions of these compound stocks in the respective cell culture medium, with a final DMSO concentration of 0.1 % (*v*/v). DMSO 0.1 % (v/v) was also added to untreated controls.

RPTEC/TERT1 cells were either treated with brequinar, positive controls, or a 0.1 % DMSO (v/v) vehicle control for 24 h (single exposure) or every 24 h for five consecutive days (repeated exposure). PHH were exposed to brequinar or vehicle control for 24 h. For the viability assays, the brequinar starting concentration was 100 μM, the maximum

achievable from a 0.1 M stock without exceeding 0.1 % DMSO, and was diluted using a 1:3 dilution factor (PHH 24 h and RPTEC/TERT1 24 h) or a 1:2 dilution factor (RPTEC/TERT1 repeated exposure). Treatment concentrations for transcriptomics and Seahorse studies were selected based on the cell viability data (Figs. 1a, 3a, and c). For a single 24-h exposure, cells were treated with brequinar at concentrations up to 100 μM. Since repeated exposure of brequinar led to significant cell death at higher concentrations, the tested concentrations for the subsequent differential gene expression studies were reduced. For repeated exposure, cells were therefore treated with 0.3, 3, and 20 μM brequinar. A phase I clinical study reported peak plasma concentrations of 166 and 217 μM in two patients on day 5 following daily treatment with the recommended 250 mg/m^2 dose for clinical phase II trials (Arteaga et al., 1989). The concentrations for sodium arsenite (10 μM) and tunicamycin (0.3 μM) were previously determined (Carta et al., 2023; Jennings et al., 2023; Niemeijer et al., 2024).

2.3. Cell viability and lactate assays

Cell viability of PHH was assessed 24 h after exposure to brequinar using the ATPlite assay (Perkin Elmer, 6016736), according to the manufacturer's instructions, as the ATP assay is often used as cell viability assay for liver models, including PHH (Bell et al., 2016; Utkarsh et al., 2016). Briefly, 100 μL/well of the reconstituted substrate solution was added to the cells and luminescence was measured in a plate reader.

Cell viability and cellular stress of RPTEC/TERT1 cells upon brequinar exposure were assessed at the end of the treatment period using the resazurin reduction and lactate assays, respectively, as previously described (Limonciel et al., 2011; van der Stel et al., 2020). The resazurin reduction assay is commonly used as an endpoint for assessing cellular viability in RPTEC/TERT1 cells (Capinha et al., 2023; van der Stel et al., 2020). In addition, measuring supernatant lactate levels provides insights into the onset of cellular stress, as elevated lactate levels often occur before cell death (Limonciel et al., 2011). Together, these assays provide valuable information on the cellular viability and stress of RPTEC/TERT1 cells. In brief, supernatant was removed and collected for the lactate assay. Note that for the repeat dose study, supernatant medium was collected every 24 h. Cells were then incubated with 100 μL/well of 44 μM resazurin in cell culture medium for 1.5 h at 36.5 °C and 5 % CO_2, after which the reduction of resazurin to resorufin was measured at excitation/emission 540/590 nm using the CLARIOstar plate reader. For the lactate assay, 10 μL of the collected supernatant was mixed with 90 μL lactate reagent mixture (consisting of 86 mM triethanolamine hydrochloride, 8.6 mM EDTA-Na_2, 34 mM $MgCl_2$, 326 μM phenazine methosulfate (PMS), 790 μM iodonitrotetrazolium chloride (INT), 7 % ethanol, 0.4 % Triton-X-100, 3.3 mM β-nicotinamide adenine dinucleotide hydrate (β-NAD), and 4 U/mL lactate dehydrogenase). After approximately 7 min optical density was measured at 490 nm using the CLARIOstar plate reader.

The raw data values for each replicate for these assays were converted to the percentage of the vehicle control, which consisted of cell culture medium with 0.1 % DMSO (*v*/v). For the resazurin reduction assay, background fluorescence (relative fluorescence units, RFU) was subtracted prior to the conversion. PHH viability assays were carried out in one experiment containing 3 biological replicates, RPTEC/TERT1 viability assays were carried out in 2–3 separate experiments, each containing at least 2–3 biological replicates.

2.4. Assessment of mitochondrial function

The mitochondrial respiration of RPTEC/TERT1 cells after a 24-h exposure to brequinar (100 μM maximum with two-fold serial dilutions down to 0.78 μM) was evaluated by measuring the cellular oxygen consumption rates (OCR) using the Seahorse XFe96 Bioanalyser (Agilent) with the MitoStress assay as previously described (van der Stel et al., 2020), with some adjustments in the injection and measurement steps. The injections only consisted of modulators which were added sequentially as follows: (A) oligomycin (2 μM), (B) FCCP (2 μM), and (C) rotenone and antimycin A (0.5 μM each). The OCR measurements were set up as follows: first the baseline OCR was measured three times, followed by three measurements for each modulator injection. After background correction, the OCR data was exported from Seahorse Wave software version 2.6.1.53 to Microsoft Excel. The basal and maximal OCR upon brequinar exposure were calculated as percentage of basal and maximal respiration of the vehicle control. For the basal respiration, the first measurement point was taken for each replicate (i.e. at 1.31 min). For the maximal respiration, the first measurement point after injection of FCCP was taken for each replicate (i.e. at 40.3 min). Seahorse assays were carried out in 2 separate experiments, each containing at least 3 biological replicates.

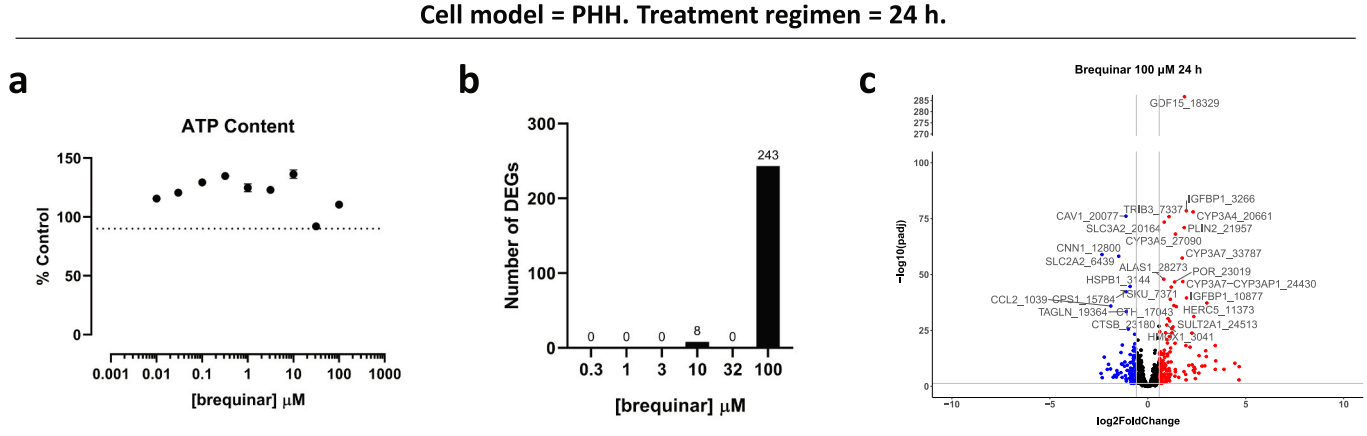

Fig. 1. Cell viability and differential gene expression in primary human hepatocytes (PHH) treated with brequinar up to 100 μM for 24 h. **a** Cell viability was assessed using the ATPlite assay. Luminescence is shown as mean ± SD (n = 3) and depicted as % control (untreated). The dotted line represents a 10 % decrease in luminescence compared to the control. Statistical significance was determined using one-way ANOVA. No significant differences were detected. **b** Overview of the number of differentially expressed genes (DEGs), represented by different probe IDs, following DESeq2 analysis in R for each tested concentration (0.3–100 μM) compared to the untreated control with cut-offs set to: average normalised read count (calculated per treatment condition) ≥ 5, padj <0.05, and log2FoldChange > |0.585| (n = 3). **c** Volcano plot illustrating the DEGs at 100 μM, with downregulated genes shown as blue dots and upregulated genes as red dots (n = 3). The top 25 significant DEGs are labelled with their gene names and probe IDs. (For interpretation of the references to colour in this figure legend, the reader is referred to the web version of this article.)

2.5. TempO-Seq transcriptomics assay

For the TempO-Seq assay, at least three replicates per condition were included. At the end of the treatment period, cells were lysed with 100 µL/well of 1× TempO-Seq Lysis buffer for 15 min at room temperature. Lysates were stored at −80 °C until they were shipped to BioClavis (Glasgow, UK) for subsequent analysis. The TempO-Seq assay was performed using the EU-ToxRisk v2.1 panel (3565 probes representing 3257 genes) for PHH and the v2.2 panel (4041 probes representing 3254 genes) for RPTEC/TERT1. Each panel was carried out in one experiment that contained 3 biological replicates. Further details of the TempO-Seq assay are described elsewhere (Limonciel et al., 2018a). The output of this analysis was presented as raw counts per probe per sample for the three datasets (i.e. PHH 24 h, RPTEC/TERT1 24 h, and RPTEC/TERT1 repeated dose toxicity (RDT) testing) (Supplementary File 1).

2.6. TempO-Seq transcriptomics data analysis and visualisation

The v2.1 (PHH) and v2.2 (RPTEC/TERT1) gene datasets were analysed separately. The two RPTEC/TERT1 datasets (24 h and RDT) were combined for further analysis. A quality control check was performed on all samples to ensure sufficient read counts, with a threshold set to 500,000 total read counts minimum. All samples passed this quality control step and were subsequently normalised and analysed for differential expression using the *DESeq2* package (Love et al., 2014) in RStudio 2023.12.1 Build 402 and R version 4.3.3 (Nunes et al., 2022). For each treatment condition, the average normalised read counts per probe were calculated. To refine the data, we applied two filters to remove probes with low counts or lack of statistical significance. Firstly, probes were removed if none of the conditions (including all treatment concentrations, exposure times, and untreated controls) had an average normalised read count of 25 or higher. Secondly, probes were removed if none of the conditions had an adjusted *p*-value (padj) lower than 0.05. The obtained output was used to generate Volcano plots and heat maps. For the heat maps and graphs displaying normalised read counts, we selected a single probe ID for each gene when multiple probe IDs were available. The selected probe ID was based on the highest sum of the absolute log2FoldChange values across all brequinar conditions. To identify differentially expressed genes (DEGs), represented by different probe IDs, additional filters were applied: probes were removed if both the untreated control group and respective treatment group (i.e. this was done for each treatment condition separately, meaning per concentration and exposure time) had 1) an average normalised read count lower than 5 to eliminate background noise; 2) a padj of 0.05 or higher to remove insignificant results; 3) a log2FoldChange between −0.585 and 0.585 to remove small fold changes with minimal biological relevance. For the Volcano plots, the above-described first filter (removal of probes with average normalised read counts below 5) was applied to remove background noise. Other R packages that were used included *tidyverse* (Wickham et al., 2019) (which includes *ggplot2* and *dplyr*), *RColorBrewer*, *circlize* (Gu et al., 2014), and *ComplexHeatmap* (Gu, 2022).

Pathway visualisation was performed through an over-representation analysis (ORA) using the ConsensusPathDB (CPDB)-human database Release 35 (http://cpdb.molgen.mpg.de/) (Herwig et al., 2016; Kamburov et al., 2011; Kamburov and Herwig, 2022). Upregulated DEGs (filtered as described above, but with log2FoldChange > 0.585) were uploaded per treatment condition as HUGO Gene Nomenclature Committee (HGNC) symbols. A background list containing all measured genes was provided as well. The option 'pathways as defined by pathway databases' was selected and default settings were used (minimum overlap with input list was 2 and p-value cut-off was 0.01). The list of identified pathways was refined as follows: 1) pathways with a q-value of 0.05 or higher (i.e. -log q-value of 1.3 or lower) were removed; 2) only pathways from the pathway sources Wikipathways, Reactome, KEGG, and PID were included; 3) pathways should present a minimum of 4 candidates and 10 % overlap; 4) in case of duplicates, the first pathway was selected; 5) irrelevant pathways were excluded, e.g. related to irrelevant organs, diseases, or drugs. The selection of target genes associated with the described stress response pathways was done using information from CPDB as well as various published papers (Carta et al., 2023; di Masi et al., 2009; Jennings et al., 2023; Jennings et al., 2013; Lim and Huang, 2008; Liu et al., 2017; Murphy et al., 2024; Wang et al., 2012; Wilmes et al., 2015). For genes related to the mitochondria, the MitoCarta3.0 human dataset was consulted (Rath et al., 2021).

2.7. Statistical analysis

Data used for statistical analysis were first converted to % control (untreated) in Microsoft Excel as described in sections 2.3 (cell viability) and 2.4 (Seahorse assay), respectively. Statistical significance was then determined using one-way ANOVA with Dunnett's multiple comparisons test in GraphPad Prism version 9.0. Data are presented as mean ± standard deviation (SD) for a minimum of *n* independent replicates given in the figure legends.

3. Results

3.1. Differential gene expression and pathway analysis in PHH

Brequinar did not reduce the viability of PHH up to 100 µM after a 24-h treatment (Fig. 1a). Exposure to 100 µM brequinar led to the highest number of DEGs in PHH with 243 in total, whereas lower concentrations showed no or relatively few alterations in gene expression levels (Fig. 1b). The top 25 most significant DEGs are illustrated in a Volcano plot (Fig. 1c). Among these are various drug-metabolising enzymes that were found to be upregulated, including Sulfotransferase Family 2 A Member 1 (*SULT2A1*) and several Cytochrome P450 (CYP) enzymes (*CYP3A4*, *CYP3A5*, and *CYP3A7*) (Fig. 1c). Other genes that were significantly upregulated include Growth Differentiation Factor 15 (*GDF15*), Tribbles Pseudokinase 3 (*TRIB3*), and Heme Oxygenase 1 (*HMOX1*) (Fig. 1c).

The upregulated DEGs were further analysed to identify stress response pathways activated in response to brequinar exposure through an over-representation analysis using the CPDB-human database. The top 15 affected pathways with the lowest q-values are shown after exposure to 100 µM brequinar (Fig. 2a). One of the pathways identified was the activation of the nuclear receptor (NR) family, specifically targeting the constitutive androstane receptor (CAR) and the pregnane X receptor (PXR) pathways (Fig. 2a), which are members of the NR1 family (Jennings et al., 2013). Moreover, brequinar induced interferon signalling pathways and the UPR (Fig. 2a). The gene expression patterns of various genes involved in xenobiotic metabolism, as well as several target genes of the Nrf2 and UPR stress response pathways, are illustrated in heat maps (Fig. 2b), whereby the colour intensities visually represent the log fold change (lfc) in gene expression relative to the untreated control condition (red hues indicate an upregulation and blue hues a downregulation). Among the most upregulated genes within the phase I and II metabolising enzyme families were enzymes from the CYP1A (*CYP1A1* and *CYP1A2*) (lfc: 3.4 and 3.5) and CYP3A (*CYP3A4*, *CYP3A5*, and *CYP3A7*) (lfc: 2.3, 2.3, and 1.8) families (Fig. 2b), which are part of the Aryl Hydrocarbon Receptor (AHR) and PXR/CAR families, respectively (di Masi et al., 2009; Jennings et al., 2013; Lim and Huang, 2008; Wang et al., 2012). Notably, the upregulation of the CYP1A enzymes occurred already at concentrations below 100 µM, indicating a sensitivity to lower concentrations. Members of the CYP2 family (*CYP2A6*, *CYP2B6*, *CYP2C8*, *CYP2C9*, and *CYP2C19*), which are targets of the PXR/CAR pathway (di Masi et al., 2009; Jennings et al., 2013; Lim and Huang, 2008; Wang et al., 2012), were also activated upon 100 µM brequinar exposure, but to a lesser extent compared to the CYP1A and CYP3A enzymes. Furthermore, 100 µM brequinar induced the expression of the phase II drug-metabolising enzymes *SULT2A1* and UDP Glucuronosyltransferase Family 1 Member A1 (*UGT1A1*). At

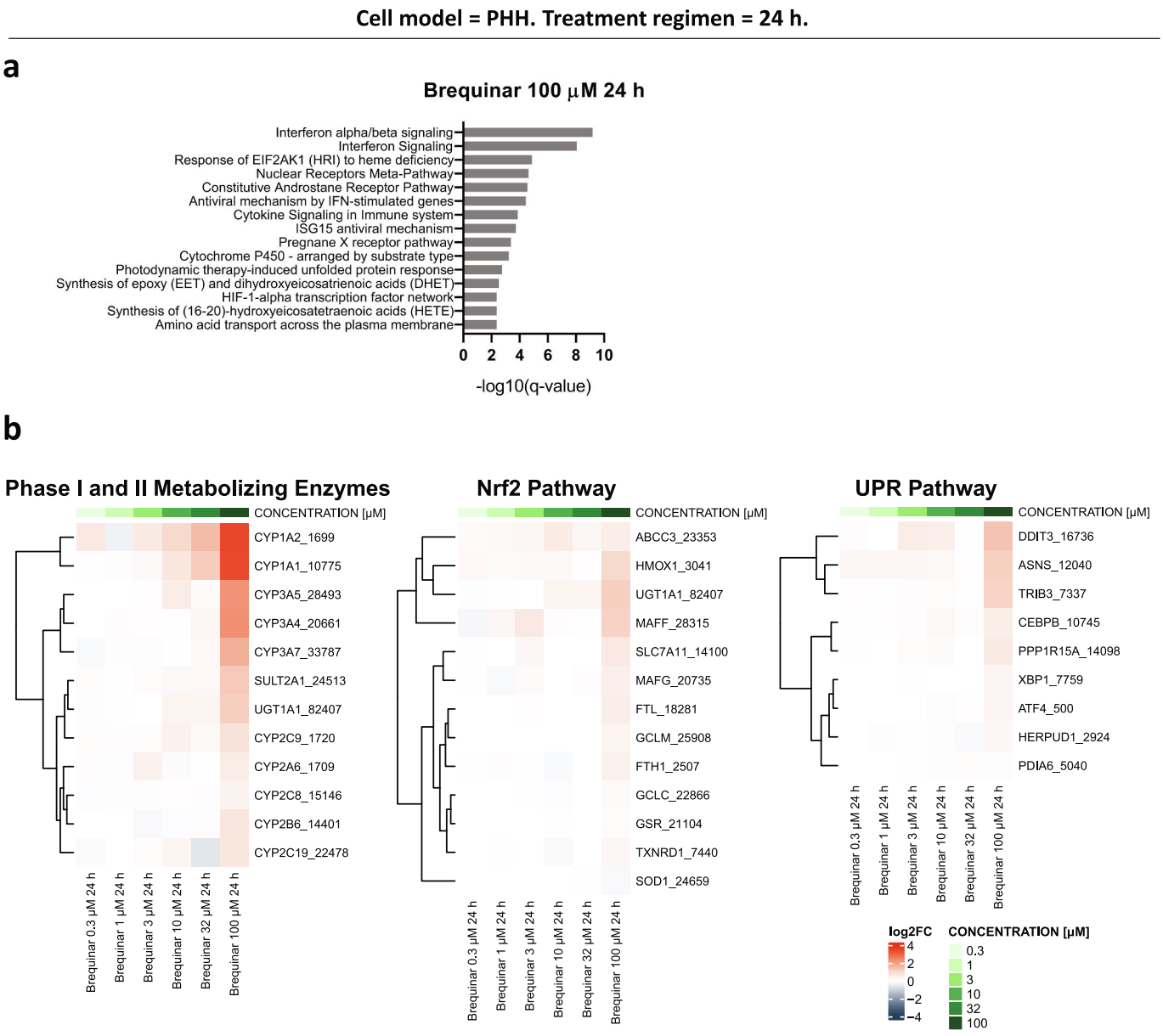

Fig. 2. Analysis of activated pathways in PHH after a single 24-h exposure to brequinar up to 100 μM. **a** Significantly altered pathways (q-value <0.05) ($n = 3$) upon 100 μM treatment were identified based on the corresponding upregulated DEGs using the over-representation analysis (ORA) tool in ConsensusPathDB. The top 15 pathways are presented with their corresponding q-values shown on a logarithmic scale. **b** Heat maps of target genes (with corresponding probe ID) involved in xenobiotic metabolism and the Nrf2 and unfolded protein response (UPR) stress response pathways. The colours visually represent the log2FoldChange (log2FC) in gene expression in response to increasing brequinar treatment (0.3–100 μM) relative to the untreated control with red indicating an increase, blue a decrease, and white no change. Genes were included if the following criteria were met at least once across all conditions: average normalised read count (calculated per treatment condition) ≥ 25 and padj <0.05 ($n = 3$). (For interpretation of the references to colour in this figure legend, the reader is referred to the web version of this article.)

concentrations below 100 μM, the overall activation of the mentioned genes—except for *CYP1A1* and *CYP1A2*—was less pronounced and did not exhibit a clear concentration-dependent pattern. Moreover, brequinar treatment resulted in the upregulation of several key genes associated with the UPR pathway, including DNA Damage Inducible Transcript 3 (*DDIT3*), Asparagine Synthetase (*ASNS*), *TRIB3*, and Protein Phosphatase 1 Regulatory Subunit 15 A (*PPP1R15A*), with the most pronounced effects observed at 100 μM (Fig. 2b). Since these genes are part of the Eukaryotic Translation Initiation Factor 2 Alpha Kinase 3 (*EIF2AK3*, otherwise known as PERK) branch, this might indicate that brequinar primarily influences this particular branch of the UPR pathway. In contrast, brequinar did not seem to affect Activating Transcription Factor 6 (*ATF6*) or DnaJ Heat Shock Protein Family Member B9 (*DNAJB9*), which are associated with other branches of the UPR. Several genes within the Nrf2 pathway were found to be upregulated to some extent, primarily at 100 μM, such as *HMOX1*, MAF BZIP Transcription Factor F (*MAFF*), Glutamate-Cysteine Ligase Modifier Subunit (*GCLM*), and Solute Carrier Family 7 Member 11 (*SLC7A11*) (Fig. 2b). Some genes of the Nrf2 pathway were not or only mildly affected by brequinar, such as Sulfiredoxin 1 (*SRXN1*), Glutamate-Cysteine Ligase Catalytic Subunit (*GCLC*), and Glutathione-Disulfide Reductase (*GSR*), as evident from the low fold changes.

3.2. Cell viability and cellular stress in RPTEC/TERT1 cells

RPTEC/TERT1 cells exposed to brequinar for 24 h showed no decrease in cell viability up to 100 μM (Fig. 3a); however, supernatant lactate was significantly increased at 100 μM (Fig. 3b). Since

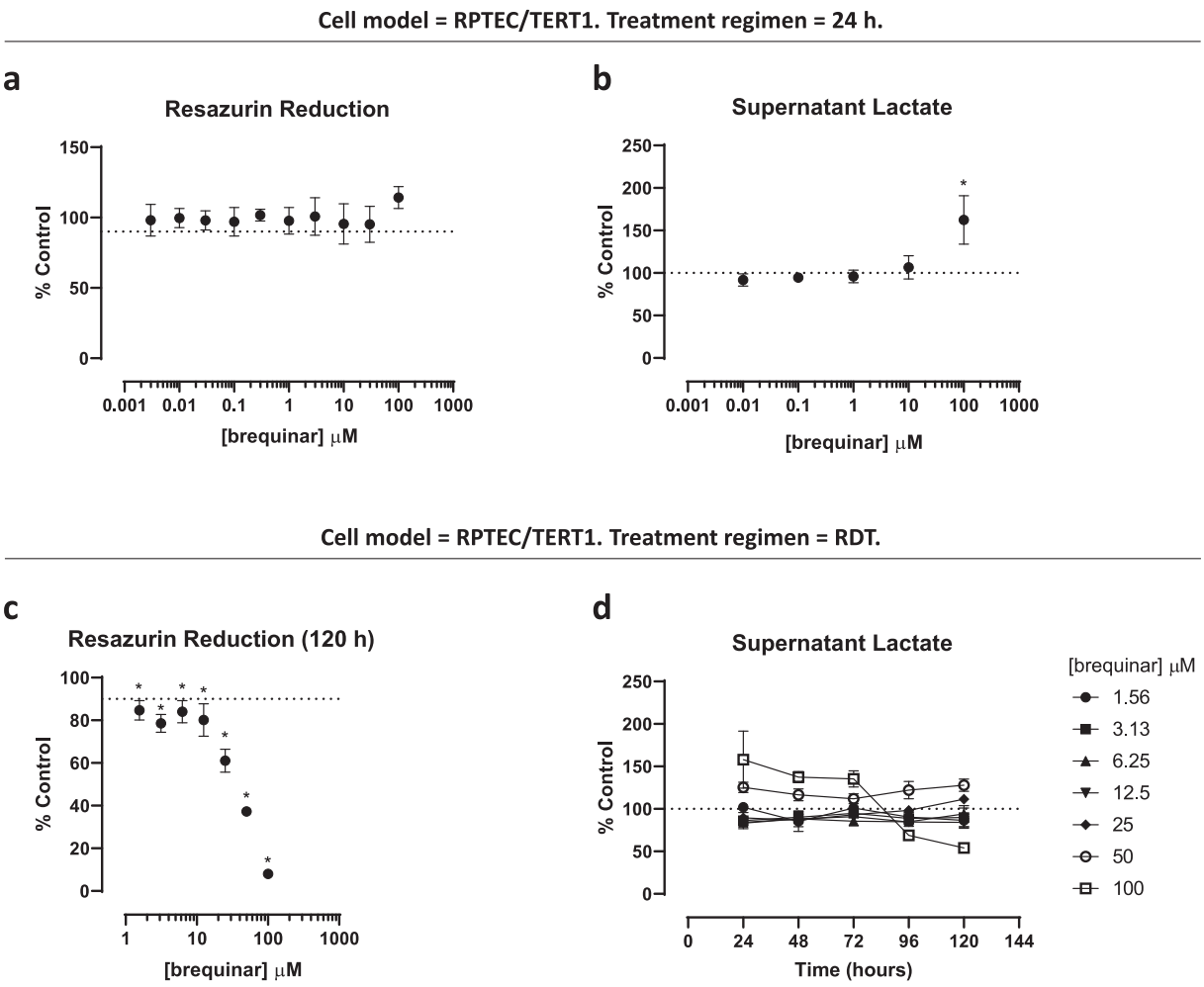

Fig. 3. Cell viability and cellular stress of RPTEC/TERT1 cells treated with brequinar for 24 h (single exposure) or every 24 h for five consecutive days (repeated dose toxicity (RDT) testing) up to 100 μM. The starting concentration of brequinar was 100 μM, which was diluted in a 1:3 series (24 h) or a 1:2 series (RDT). For the 24 h supernatant lactate measurement only 0.01, 0.1, 1, 10, and 100 μM are shown. **a and c** Cell viability results are shown in (**a**) and (**c**) for 24 h and RDT, respectively. Cell viability was measured by resazurin reduction at the end of the treatment period. Data is shown as mean ± SD ($n = 4$ for 24 h and $n = 6$ for RDT) and depicted as % control (untreated). Statistical significance was calculated using one-way ANOVA with * representing a p-value <0.05 (untreated versus treated) and ≥ IC_{10}. The dotted line represents a decrease of 10 % in resazurin reduction compared to the control. **b and d** Supernatant lactate was measured after 24 h (**b**) or every 24 h for RDT (**d**). Data is shown as mean ± SD ($n = 3$ for both, for RDT these were technical replicates) and depicted as % control (untreated). Statistical significance was calculated using one-way ANOVA with * representing a p-value <0.05 (untreated versus treated). Each treatment was paired with its corresponding untreated time-matched control. Statistics are not shown in (**d**); 100 μM significantly changed supernatant lactate at all timepoints and 50 μM on days 2, 4, and 5.

differentiated RPTEC/TERT1 cells exhibit an oxidative phenotype upon maturation (Aschauer et al., 2013), elevated supernatant lactate levels are an indication of increased glycolysis rates and therefore serve as a marker of induced cellular stress (Limonciel et al., 2011). Lactate measured in the cell supernatant is hence a sensitive marker that is elevated at concentrations prior to cell death. Daily repeated exposure of RPTEC/TERT1 cells to brequinar over a treatment period of five consecutive days (120 h total) resulted in a significant concentration-dependent decrease in cell viability (Fig. 3c). Supernatant lactate levels remained largely unaffected at concentrations up to 25 μM (Fig. 3d). In contrast, 50 μM brequinar treatment showed increased supernatant lactate levels throughout the entire treatment period, and 100 μM brequinar treatment led to increased supernatant lactate levels during the first three days of treatment, reflecting cell stress; supernatant lactate levels dropped on days 4 and 5, most likely due to subsequent cell death that was confirmed on day 5 by the resazurin assay (Fig. 3c and d).

3.3. *Differential gene expression and pathway analysis in RPTEC/TERT1 cells*

The highest number of DEGs resulted from the exposure of RPTEC/TERT1 cells to 30 and 100 μM brequinar for 24 h, with 1017 and 1067 DEGs, respectively (Fig. 4a). Lower concentrations ranging from 0.3 to 10 μM induced only modest changes in gene expression after a 24-h exposure (Fig. 4a). In contrast, repeated exposure to brequinar greatly increased the number of DEGs already at 0.3 and 3 μM (Fig. 4a), indicating a more substantial impact with prolonged exposure at lower concentrations. The DEGs are visualised in Volcano plots (Fig. 4b and c), with the most significantly up- and downregulated genes annotated. Even though exposure to 0.3 and 1 μM brequinar for 24 h resulted in relatively few gene alterations, one notable change was the upregulation of Lipocalin 2 (*LCN2*, also known as NGAL) (Fig. 4b), which is a clinical biomarker for the detection of acute kidney injury (AKI) (Devarajan, 2008). After treatment with higher concentrations for 24 h, more significantly altered genes were observed, including Amphiregulin (*AREG*), Growth Arrest And DNA Damage Inducible Alpha (*GADD45A*), and *ASNS* (Fig. 4b). These genes also appeared with the repeated

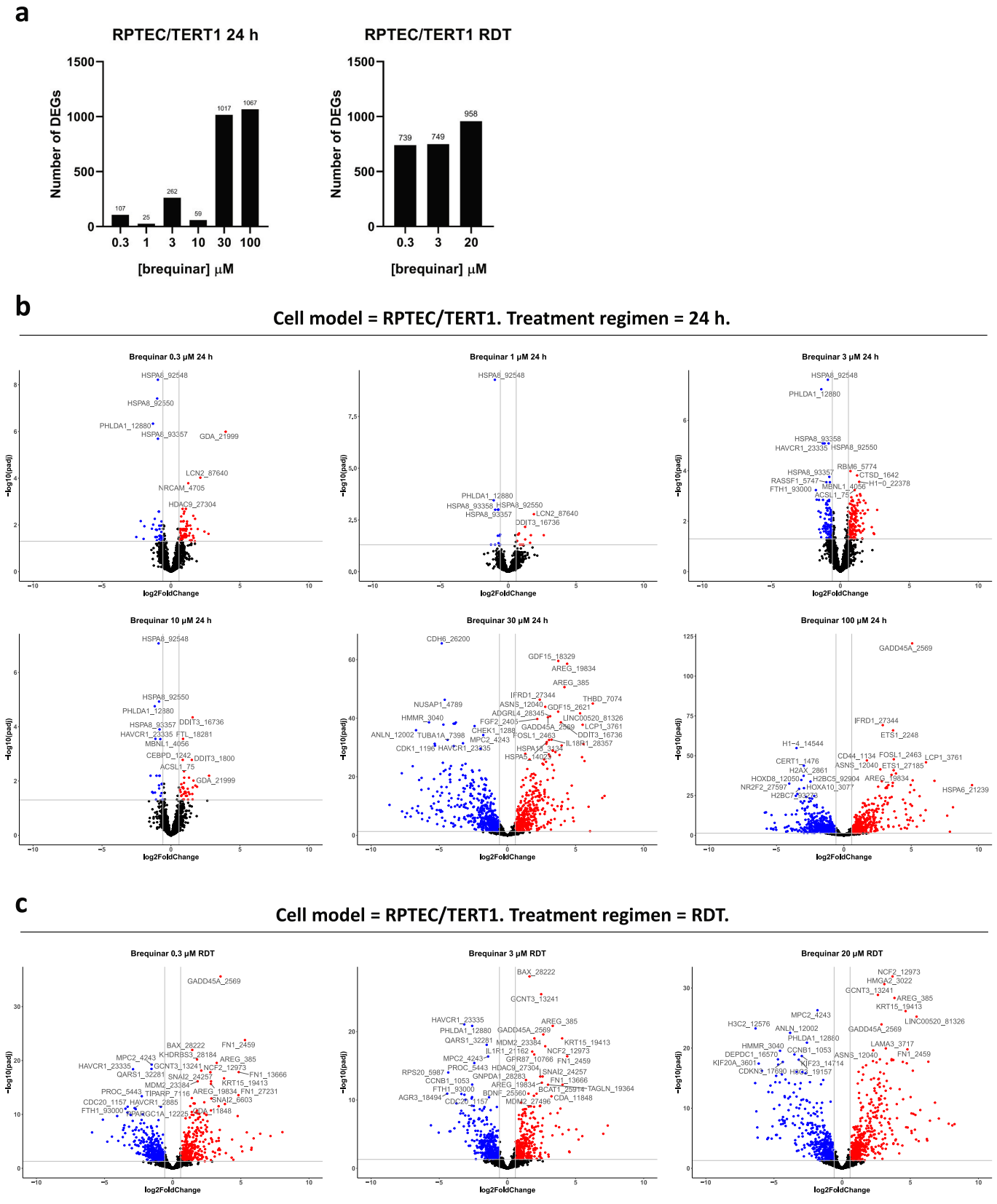

Fig. 4. Differential gene expression in RPTEC/TERT1 cells treated with brequinar for 24 h (single exposure) (0.3–100 μM) or every 24 h for five consecutive days (repeated dose toxicity (RDT) testing) (0.3, 3, and 20 μM). **a** Overview of the number of differentially expressed genes (DEGs), represented by different probe IDs, following DESeq2 analysis in R for each tested concentration compared to the corresponding untreated time-matched control with cut-offs set to: average normalised read count (calculated per treatment condition) ≥ 5, padj <0.05, and log2FoldChange > |0.585| ($n = 3$). **b and c** Volcano plots illustrating the DEGs for 24 h (**b**) and RDT (**c**), respectively, with downregulated genes shown as blue dots and upregulated genes as red dots ($n = 3$). Depending on the available space, the plots label up to the top 30 significant DEGs with gene names and probe IDs. (For interpretation of the references to colour in this figure legend, the reader is referred to the web version of this article.)

treatment regimen along with BCL2 Associated X (*BAX*), Snail Family Transcriptional Repressor 2 (*SNAI2*), and Mouse Double Minute 2 (*MDM2*), to name a few (Fig. 4c). A detailed comparative analysis of the changes in gene expression between the different treatment conditions is described below.

The response of RPTEC/TERT1 cells to brequinar exposure was also investigated by analysing the upregulated DEGs using the CPDB-human database to evaluate pathway activation. The top 15 most significant pathways, ranked by their q-values, are presented in Fig. 5. This analysis revealed differences in point of departures of stress response pathway activation between single and repeated administrations of brequinar. After a single 24-h exposure, stress response pathways were identified at 10, 30, and 100 μM, whereas no significant pathways could be detected at 0.3, 1, and 3 μM brequinar treatment. Nonetheless, several stress response pathways were identified at 0.3 and 3 μM with repeated dosing, as well as at 20 μM. One of the most prominent stress response pathways that was induced by brequinar across all these conditions was the UPR (Fig. 5). In addition, the 24-h exposure at 100 μM led to the activation of several eukaryotic translation events (e.g. 'GTP hydrolysis and joining of the 60S ribosomal subunit', 'translation initiation', 'formation of a pool of free 40S subunits', and 'peptide chain elongation') (Fig. 5) that also appeared after a repeated exposure of RPTEC/TERT1 cells to the known UPR-inducer tunicamycin at 0.3 μM (Fig. S1). Besides the UPR, brequinar also induced an inflammatory response for all above-mentioned conditions except for the 24-h exposure at 10 μM, as reflected by the activation of signalling pathways involving interleukins (ILs), Nuclear Factor Kappa B (NF-κB), and Tumour Necrosis Factor (*TNF*) (Fig. 5). Notably, repeated exposure to brequinar at all three tested concentrations resulted in significant activation of the p53 pathway (Fig. 5). Furthermore, activation of the Nrf2 pathway became apparent after repeated exposure at 20 μM (Fig. 5). Both the p53 and Nrf2 pathways were also detected after a 24-h exposure at 30 μM, while only p53

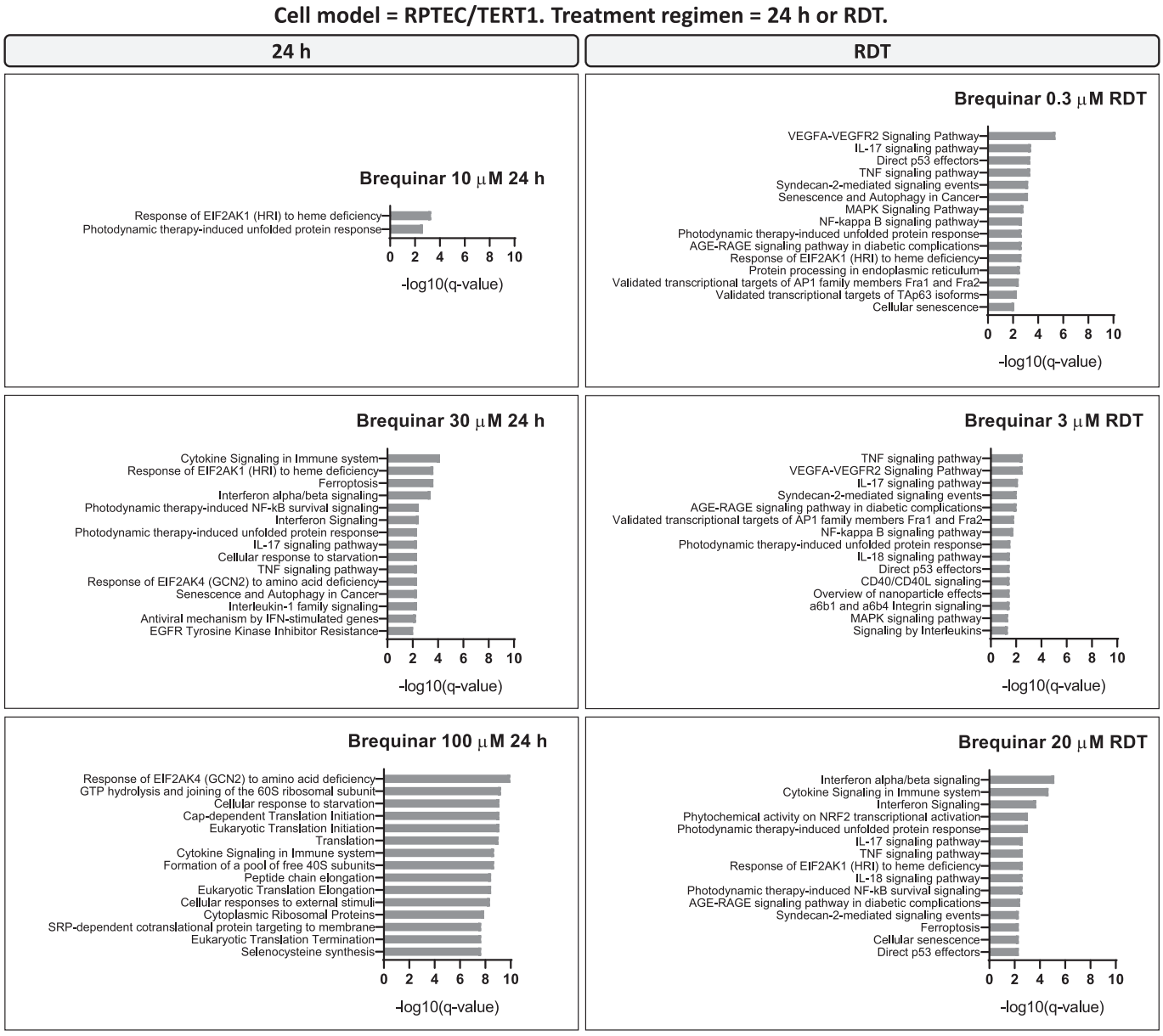

Fig. 5. Analysis of activated pathways in RPTEC/TERT1 cells treated with brequinar for 24 h (single exposure) (10, 30, and 100 μM) or every 24 h for five consecutive days (repeated dose toxicity (RDT) testing) (0.3, 3, and 20 μM). Significantly altered pathways (q-value <0.05) ($n = 3$) for each treatment condition were identified based on the corresponding upregulated DEGs using the ORA tool in ConsensusPathDB. No significant pathways could be identified at 0.3, 1, and 3 μM brequinar treatment after a single 24 h exposure. The top 15 pathways are presented with their corresponding q-values shown on a logarithmic scale.

was observed at 100 μM; however, these instances were less significant (−log q-values: 1.7, 1.5, and 2.0, respectively) compared to the activation seen under repeated dosing conditions.

In addition to the ORA, the effects of brequinar were also analysed at the gene level. The findings are illustrated in Fig. 6, which displays the gene expression changes (in lfc relative to the untreated control) for key genes associated with the stress response pathways above. The impact of brequinar on UPR activation was particularly evident at the gene level, as demonstrated by the overall upregulation of many key genes (Fig. 6), which represent the three distinct branches of the UPR pathway: *EIF2AK3* (PERK), *ATF6*, and Endoplasmic Reticulum To Nucleus Signalling 1 (*ERN1*, aka IRE1) (Jennings et al., 2013). Among the most prominently upregulated genes were *DDIT3*, *TRIB3*, *ASNS*, *DNAJB9*, X-Box Binding Protein 1 (*XBP1*), *PPP1R15A*, and Heat Shock Protein Family A Member 5 (*HSPA5*). Furthermore, brequinar upregulated several genes associated with the Nrf2 pathway, such as *HMOX1*, *SLC7A11*, Thioredoxin Reductase 1 (*TXNRD1*), *MAFF*, and Ferritin Light Chain (*FTL*) (Fig. 6). *HMOX1* was only upregulated at concentrations of 30 and 100 μM after a single 24-h exposure and across all concentrations following repeated exposure, demonstrating that lower concentrations of brequinar with a single administration were insufficient to upregulate *HMOX1*. An opposite pattern was observed for Ferritin Heavy Chain 1 (*FTH1*), which was upregulated after a 24-h exposure but down-regulated following repeated exposure. For other genes, such as NAD(*P*)

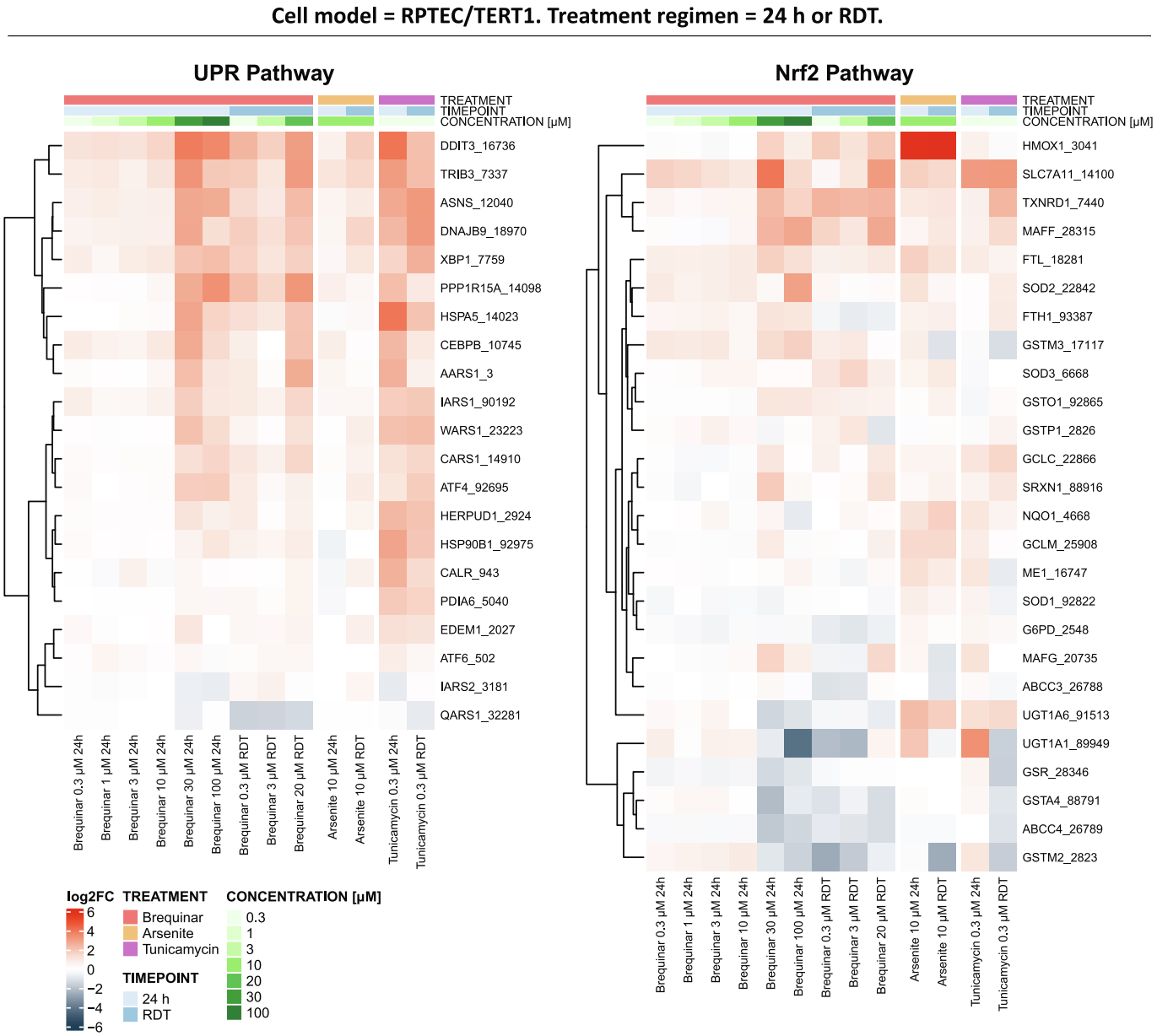

Fig. 6. Activation of stress response pathways at the gene level in RPTEC/TERT1 cells treated with brequinar for 24 h (single exposure) (0.3–100 μM) or every 24 h for five consecutive days (repeated dose toxicity (RDT) testing) (0.3, 3, and 20 μM). The heat maps visually represent the log2FoldChange (log2FC) in gene expression for target genes associated with the UPR, Nrf2, p53, and inflammatory responses in response to increasing brequinar treatment compared to the corresponding untreated time-matched control (red: increased expression, blue: decreased expression, and white: no change). Sodium arsenite and tunicamycin were used as positive controls for Nrf2 and UPR, respectively. Each heat map displays the following conditions from left to right: brequinar 24 h 0.3–100 μM, brequinar RDT 0.3–20 μM, 10 μM sodium arsenite 24 h and RDT, and 0.3 μM tunicamycin 24 h and RDT. Genes were included if the following criteria were met at least once across all conditions: average normalised read count (calculated per treatment condition) ≥ 25 and padj <0.05 ($n = 3$). (For interpretation of the references to colour in this figure legend, the reader is referred to the web version of this article.)

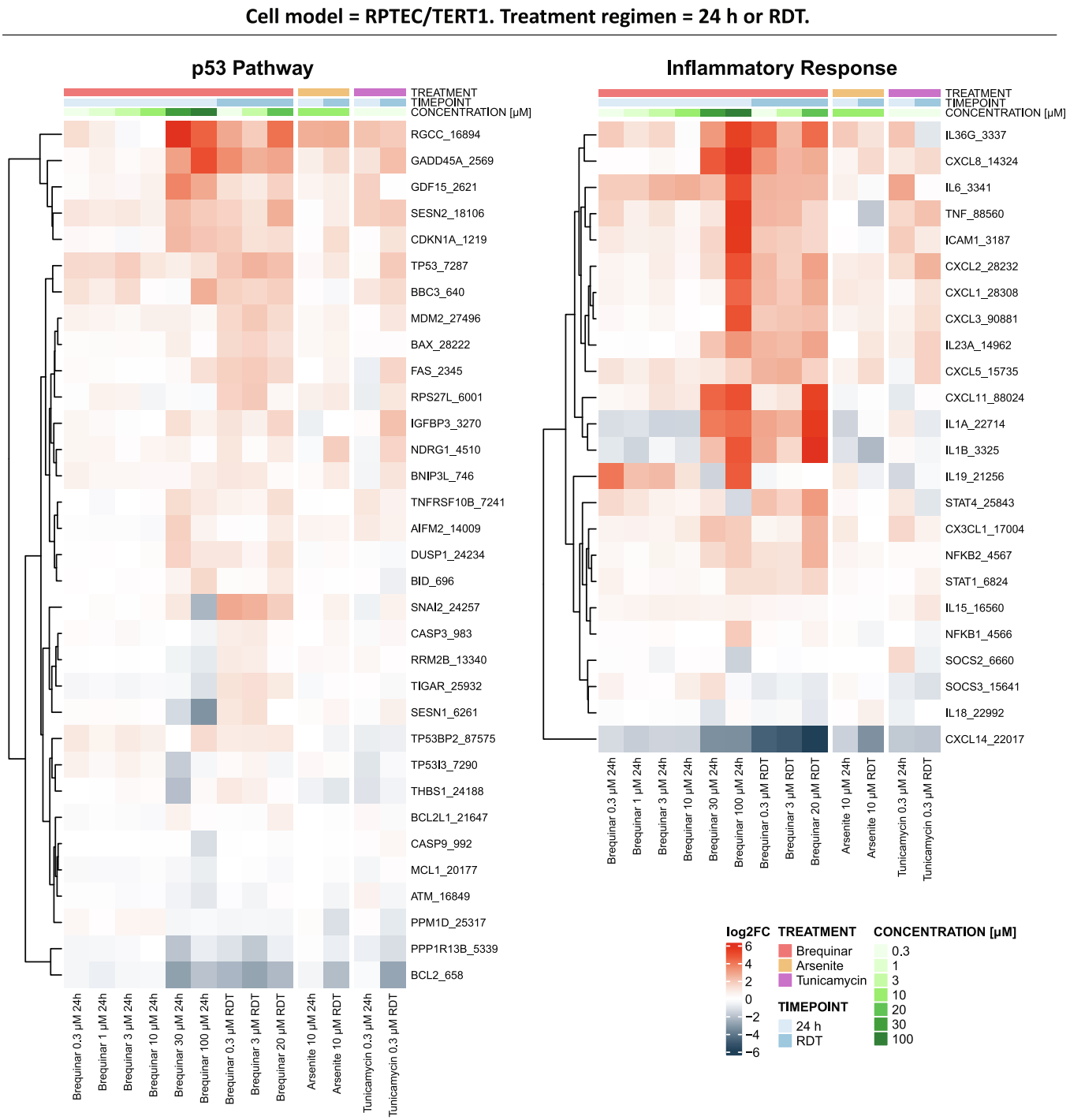

Fig. 6. (*continued*).

H Quinone Dehydrogenase 1 (*NQO1*) and *GCLM*, the effects of brequinar were more variable and less pronounced. Brequinar exposure also led to increased expression of Tumour Protein P53 (*TP53*) and alterations in the expression of genes associated with the p53 pathway (Fig. 6). Several p53 pathway-related genes were significantly upregulated after a 24-h exposure at 30 and 100 µM and following repeated exposure, including *Regulator Of Cell Cycle* (*RGCC*), *GADD45A*, *GDF15*, Sestrin 2 (*SESN2*), and Cyclin Dependent Kinase Inhibitor 1 A (*CDKN1A*, also known as p21) (Fig. 6). This upregulation was accompanied by a marked downregulation of B-Cell Lymphoma-2 (*BCL2*). Moreover, brequinar triggered an inflammatory response, as evidenced by changes in the expression of key inflammatory markers (Fig. 6). After 24 h of exposure, 100 µM brequinar resulted in the greatest upregulation of various genes, including cytokines (different ILs and *TNF*), various CXC family chemokines, and Intercellular Adhesion Molecule 1 (*ICAM1*). Repeated exposure also led to an upregulation of these genes.

Sensitivity differences in gene expression activation were observed across the stress response pathways between single and repeated exposures to brequinar. Specifically, at a lower concentration of brequinar (0.3 µM), repeated exposure resulted in a greater gene upregulation compared to a single exposure. Fig. 7 illustrates the gene expression (normalised read counts) of several target genes under these conditions. Compared to the respective untreated control group, a single exposure to 0.3 µM brequinar did not significantly alter the expression of most genes

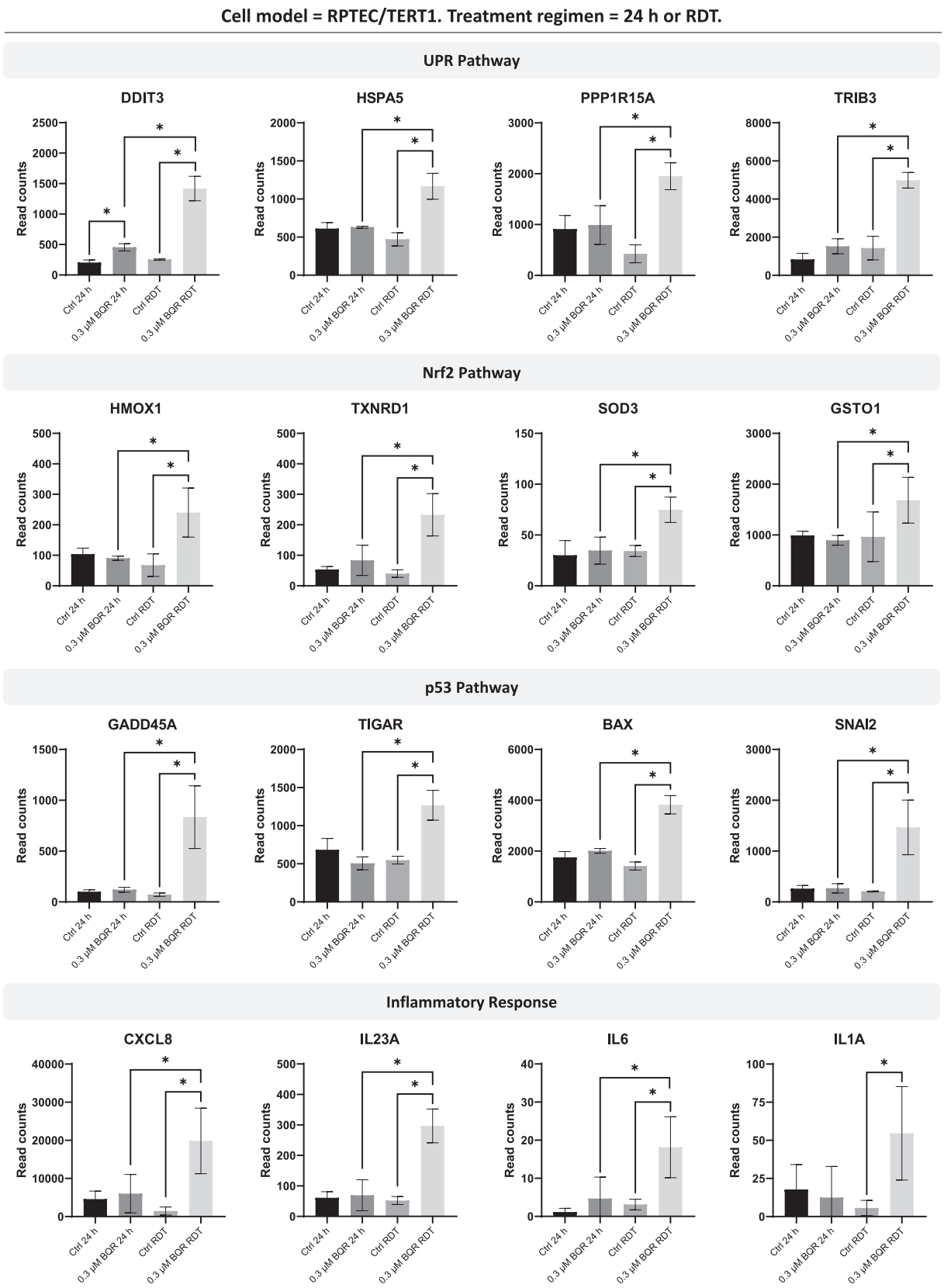

Fig. 7. Normalised read counts of selected target genes associated with the UPR, Nrf2, p53, and inflammatory responses in RPTEC/TERT1 cells treated with 0.3 µM brequinar (BQR) for 24 h (single exposure) or every 24 h for five consecutive days (repeated dose toxicity (RDT) testing). The corresponding normalised read counts for the untreated time-matched controls (Ctrl 24 h and Ctrl RDT) are also displayed for comparison. One-way ANOVA was performed to compare each treatment regimen with its respective untreated time-matched control and to compare the two treatment regimens with one another. * represents a p-value <0.05 ($n = 3$).

(Fig. 7). However, with repeated exposure, there was a significant increase in gene expression relative to both the respective untreated control and single exposure groups (Fig. 7). For instance, while a 24-h exposure to 0.3 μM brequinar caused minimal changes or even downregulation of various genes within the p53 pathway, repeated exposure led to clear upregulation. This trend was evident for various genes within this pathway such as *GADD45A*, *CDKN1A*, *BAX*, Fas Cell Surface Death Receptor (*FAS*), *SNAI2*, Caspase 3 (*CASP3*), Ribonucleotide Reductase Regulatory TP53 Inducible Subunit M2B (*RRM2B*), TP53 Induced Glycolysis Regulatory Phosphatase (*TIGAR*, aka C12orf5), and Sestrin 1 (*SESN1*), as demonstrated by both the visual fold changes and the read counts in Figs. 6 and 7, respectively. In addition to the p53 pathway, certain genes within the Nrf2 pathway, including *HMOX1*, *TXNRD1*, *MAFF*, Superoxide Dismutase 3 (*SOD3*), and Glutathione S-Transferase Omega 1 (*GSTO1*), also exhibited a more pronounced upregulation with repeated exposure compared to single exposure (Figs. 6 and 7). Similarly, genes within the UPR pathway, such as *DDIT3*, *HSPA5*, *PPP1R15A*, *TRIB3*, *DNAJB9*, and Activating Transcription Factor 4 (*ATF4*), followed the same trend (Figs. 6 and 7). A significant increase in gene expression between the untreated control and 0.3 μM brequinar treatment after a single exposure was observed for the UPR gene *DDIT3*; however, the change was less pronounced than with the repeated exposure (Fig. 7).

3.4. Downregulation of renal proximal tubule and mitochondrial gene expression

Brequinar impacted several genes associated with the renal proximal tubule phenotype (Fig. 8). For instance, Gamma-Butyrobetaine Hydroxylase 1 (*BBOX1*) emerged as one of the most downregulated genes in response to brequinar exposure. This gene is commonly downregulated in response to chemical-induced stress in RPTEC/TERT1 cells (Limonciel et al., 2018a; Wilmes et al., 2013, 2015). Similarly, the tight junction protein Claudin 2 (*CLDN2*) was also downregulated, a response that has been documented previously in proximal tubule cells upon induced stress (Limonciel et al., 2012; Wilmes et al., 2014). Gamma-Glutamyltransferase 1 (*GGT1*) is another gene that is highly expressed in RPTEC/TERT1 cells (Capinha et al., 2023; Limonciel et al., 2018a), and was found to be downregulated following repeated exposure to brequinar. Lastly, *LCN2* expression remained upregulated throughout all tested conditions, suggesting that brequinar exposure can inflict damage to the proximal tubular epithelium.

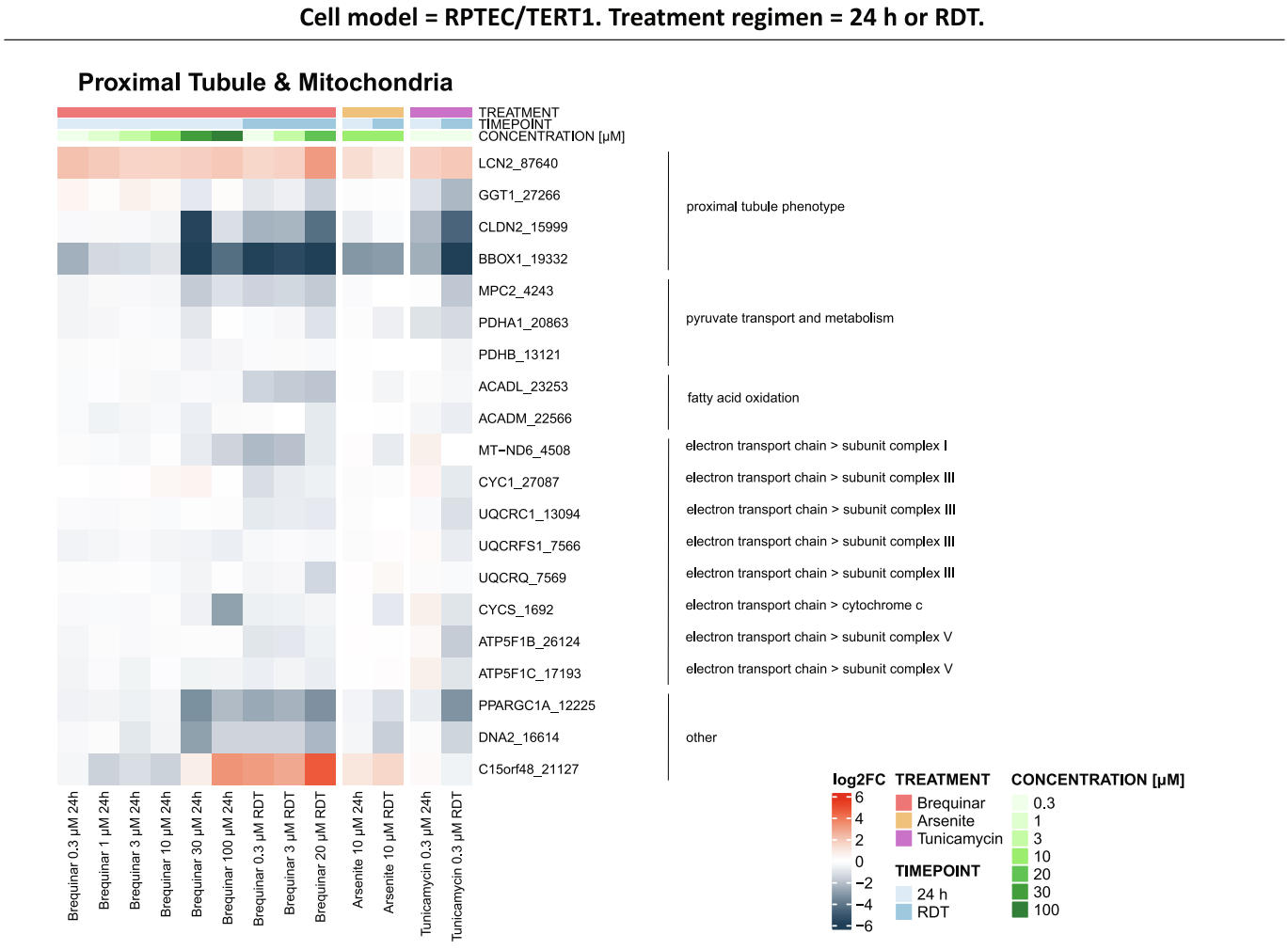

Fig. 8. Effect of brequinar on the expression of various renal proximal tubule and mitochondrial genes in RPTEC/TERT1 cells treated for 24 h (single exposure) (0.3–100 μM) or every 24 h for five consecutive days (repeated dose toxicity (RDT) testing) (0.3, 3, and 20 μM). The heat map visually represents the log2FoldChange (log2FC) in gene expression in response to increasing brequinar treatment compared to the corresponding untreated time-matched control (red: increased expression, blue: decreased expression, and white: no change). The following conditions are displayed from left to right: brequinar 24 h 0.3–100 μM, brequinar RDT 0.3–20 μM, 10 μM sodium arsenite 24 h and RDT, and 0.3 μM tunicamycin 24 h and RDT. Genes were included if the following criteria were met at least once across all conditions: average normalised read count (calculated per treatment condition) ≥ 25 and padj <0.05 ($n = 3$). (For interpretation of the references to colour in this figure legend, the reader is referred to the web version of this article.)

In addition, brequinar decreased a variety of genes involved in mitochondrial processes, which was mostly clear for a single exposure at 30 and 100 μM or following repeated exposure (Fig. 8). These include genes encoding proteins related to pyruvate transport and metabolism (such as Mitochondrial Pyruvate Carrier 2 (*MPC2*) and Pyruvate Dehydrogenase E1 Subunit Alpha 1 (*PDHA1*)), fatty acid oxidation (including Acyl-CoA Dehydrogenase Long Chain (*ACADL*)), and various (sub)units of the electron transport chain (e.g. Cytochrome C1 (*CYC1*), Ubiquinol-Cytochrome C Reductase Core Protein 1 (*UQCRC1*), Ubiquinol-Cytochrome C Reductase Complex III Subunit VII (*UQCRQ*), and Cytochrome C (*CYCS*)). Notably, there was a significant downregulation of Peroxisome Proliferator-Activated Receptor Gamma Coactivator 1 Alpha (*PPARGC1A*, also known as PGC-1α), which is a known regulator of mitochondrial biogenesis (Garcia et al., 2017). Another downregulated gene was DNA Replication Helicase/Nuclease 2 (*DNA2*), which plays a role in the replication and repair of mitochondrial DNA (Zheng et al., 2008). Interestingly, Chromosome 15 Open Reading Frame 48 (*C15orf48*) expression shifted from downregulation at 0.3–10 μM (24 h) to slight upregulation at 30 μM (24 h) and more significant upregulation at 100 μM (24 h), with further upregulation observed upon repeated dosing. *C15orf48* has been reported to reduce the mitochondrial membrane potential and intracellular ATP levels, and may induce an oxidative stress response by increasing intracellular levels of glutathione (Takakura et al., 2024).

3.5. Effect of Brequinar on mitochondrial respiration of RPTEC/TERT1 cells

To further investigate the impact of brequinar on mitochondrial function, we measured the OCR of RPTEC/TERT1 cells after a 24-h exposure to brequinar using the Seahorse MitoStress assay. By the sequential addition of specific modulators of the electron transport chain, key parameters of the mitochondrial function can be assessed through direct measurement of the OCR (van der Stel et al., 2020). Fig. 9a presents the OCR profiles of untreated (black line) and brequinar-treated (blue lines) RPTEC/TERT1 cells after 24 h. The first three data points represent the baseline OCR, which drops after addition of the modulator oligomycin to measure ATP production. Next, the uncoupler FCCP is added to reveal the maximal respiration capacity. Finally, a mixture of rotenone and antimycin A shuts down mitochondrial respiration to allow measurement of non-mitochondrial respiration. For further interpretation, the basal and maximal respiration rates following brequinar treatment were assessed and compared to the untreated control (Fig. 9b). The results revealed a marked reduction in both basal and maximal respiration rates upon brequinar exposure (Fig. 9b). Importantly, these changes in mitochondrial respiration occurred without affecting the viability of these cells after 24 h of exposure (Fig. 3a). These findings collectively suggest that brequinar can impair the mitochondrial function of RPTEC/TERT1 cells.

4. Discussion

This study highlighted different sensitivities and points of departures in the PHH and the RPTEC/TERT1 cell line in response to brequinar treatment. While exposure of PHH to 100 μM brequinar for 24 h activated the UPR and Nrf2 stress response pathways, this upregulation was substantially less pronounced compared to RPTEC/TERT1 cells. RPTEC/TERT1 cells already showed a strong activation of these pathways in response to 30 μM brequinar treatment. Notably, we observed a significant upregulation of the PXR/CAR pathway in PHH as well as of the AHR-controlled CYP1A enzymes *CYP1A1* and *CYP1A2* that play a role in xenobiotic metabolism and detoxification processes (di Masi et al., 2009; Jennings et al., 2013). This upregulation may explain the reduced sensitivity of PHH to brequinar. While several studies have proposed that brequinar undergoes hepatic metabolism, the specific CYPs involved have not yet been identified (Cosenza et al., 1993; Joshi et al., 1997; Makowka et al., 1993). Our transcriptomics analysis points to several phase I and phase II drug-metabolising enzymes as potential contributors, including members of the CYP1A and CYP3A families. Nevertheless, these findings are based solely on gene expression data. Further research is needed to assess the functional activities of these enzymes.

In contrast to PHH, RPTEC/TERT1 cells treated with brequinar exhibited a stronger upregulation of a range of genes associated with various stress response pathways, including UPR, Nrf2, p53, and inflammatory responses. The activation of the UPR stress response pathway was one of the most predominant responses observed. The increased sensitivity to UPR activation might be related to the event of brequinar-induced mitochondrial dysfunction. Notably, the UPR pathway was recently demonstrated to be the most affected stress response pathway in RPTEC/TERT1 cells upon inhibition of the electron transport chain (Carta et al., 2023). We also observed that brequinar

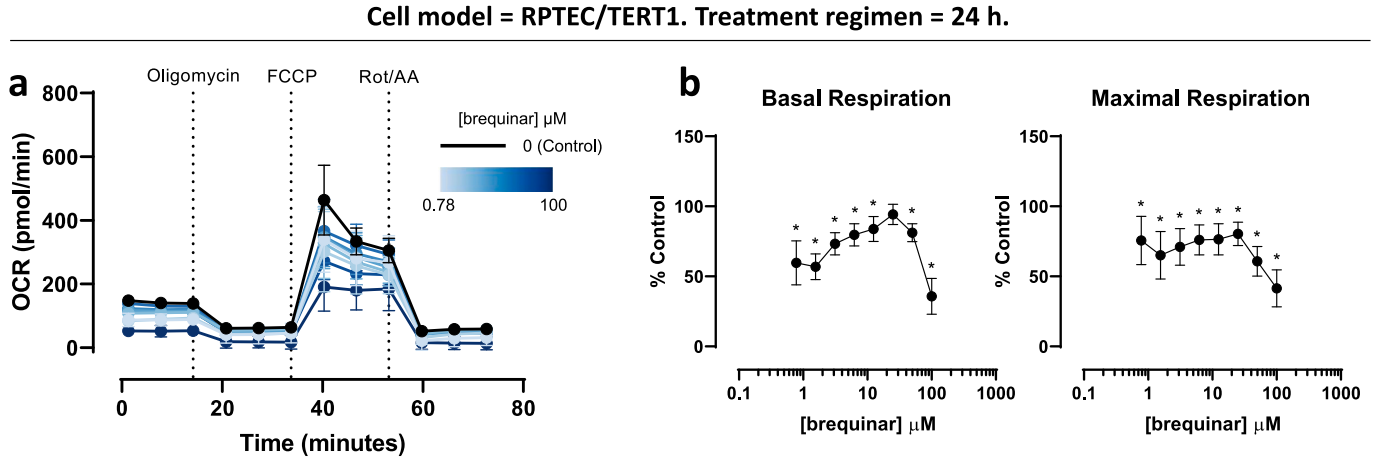

Fig. 9. Impact of brequinar on mitochondrial respiration of RPTEC/TERT1 cells following a single 24-h exposure to a range of concentrations (100 μM maximum with two-fold serial dilutions down to 0.78 μM). Mitochondrial respiration was assessed by measuring the oxygen consumption rates (OCR) using the Seahorse MitoStress assay. The complete OCR profiles of untreated (black) and treated (blue colour gradient from light to dark indicating increasing concentrations) RPTEC/TERT1 cells. The dotted lines indicate the injection times of the different modulators: oligomycin, FCCP, and rotenone together with antimycin A. The basal and maximal respiration rates of RPTEC/TERT1 cells upon brequinar treatment. Data is shown as mean ± SD ($n = 6$) and depicted as % control (untreated). Statistical significance was calculated using one-way ANOVA with * representing a p-value <0.05 (untreated versus treated). (For interpretation of the references to colour in this figure legend, the reader is referred to the web version of this article.)

exposure could induce the p53 pathway in RPTEC/TERT1 cells. Earlier studies indicate that the p53 pathway can be activated by the depletion of pyrimidine nucleotide pools (Khutornenko et al., 2010; Ladds et al., 2018; Linke et al., 1996). Ladds et al. demonstrated that brequinar-induced activation of p53 could be reversed by the concurrent addition of uridine (Ladds et al., 2018). Moreover, Khutornenko et al. reported that inhibition of complex III of the mitochondrial electron transport chain led to reduced intracellular pyrimidine nucleotide pools and activated the p53 response, which could also be prevented by uridine supplementation (Khutornenko et al., 2010). Complex III dysfunction can impair the generation of ubiquinone, which in turn may lead to the inhibition of DHODH (Banerjee et al., 2022). These studies collectively support that brequinar-induced activation of the p53 pathway is associated with pyrimidine nucleotide depletion caused by the inhibition of DHODH.

Given the unique localisation of human DHODH within the inner mitochondrial membrane and the functional linkage with the electron transport chain through ubiquinone, we investigated whether the DHODH inhibitor brequinar could impair mitochondrial function. Previously, brequinar has been shown to induce mitochondrial toxicity in two liver models, the cancer cell lines HepaRG and HepG2 (Jones et al., 2021). Here, differentiated RPTEC/TERT1 cells showed a significant reduction in both basal and maximal respiration rates after a 24-h exposure to brequinar up to 100 μM. Furthermore, brequinar was found to downregulate a variety of genes involved in mitochondrial processes, including those involved in substrate metabolism or transport and components of the electron transport chain. In addition, the gene *PPARGC1A*, which is recognised as a master regulator of mitochondrial biogenesis (Fontecha-Barriuso et al., 2020; Garcia et al., 2017), was downregulated by brequinar. This downregulation is consistent with other studies where silencing of *PPARGC1A* resulted in decreased oxygen consumption rates (LaGory et al., 2015; Rosales et al., 2019). Low *PPARGC1A* levels have also been observed in nephrotoxic AKI with a concomitant increase in *LCN2* (Fontecha-Barriuso et al., 2019; Stallons et al., 2014). Similarly, we observed elevated *LCN2* levels in RPTEC/TERT1 cells exposed to brequinar under all tested conditions, suggesting a potential link to nephrotoxicity. Additionally, brequinar exposure resulted in the significant downregulation of several highly expressed genes in RPTEC/TERT1 cells, including *BBOX1*, *CLDN2*, and *GGT1*, indicating a potential disruption of the differentiated phenotype of proximal tubular epithelial cells.

In the present study, we implemented repeated dose testing since this more accurately reflects the real-life drug administration scenarios compared to single dose exposure. Many in vitro studies, however, do not include repeated dosing, often due to the lack of stability of certain in vitro systems over longer times in culture. RPTEC/TERT1 cells are ideal for repeat dose studies due to their transcriptomic stability once the epithelium is contact-inhibited and fully matured (Aschauer et al., 2015; Limonciel et al., 2018b; Secker et al., 2019; Wilmes et al., 2015; Wilmes et al., 2013). Matured RPTEC/TERT1 cells become fully quiescent in the G0/G1 phase of the cell cycle and no longer proliferate unless they are subcultured again (Aschauer et al., 2013). In contrast, cancer cell lines often lack contact inhibition and continue to proliferate and hence show alterations in genes involved in cell cycle over the time course of longer exposure times. Another challenge for longer experiments using primary cells is that they often dedifferentiate and lose cell type-specific characteristics over time (Heslop et al., 2017), for example CYP450 enzyme activity rapidly declines in PHH in monolayer cultures. In exploring the most optimal dosing schedule for brequinar in clinical settings, several studies suggested that continuous or more frequent administration of brequinar could improve its antitumour activity (Peters et al., 1987; Schwartsmann et al., 1988). Nonetheless, an increased dosing frequency may also elevate the risk of toxicity due to sustained DHODH enzyme inhibition (Peters et al., 1990). This was exemplified by a phase I clinical study which reported that toxicity occurred at lower doses when brequinar was administered more frequently, i.e. twice weekly compared to once weekly (Bork et al., 1989). This observation is consistent with our results. We observed that repeated administration of brequinar at lower concentrations, e.g. 0.3 μM, resulted in a more pronounced induction of stress response pathways in RPTEC/TERT1 cells compared to a single exposure. Repeated exposure thus may uncover pathway activations that are not evident with single dose exposure at lower concentrations, which highlights the importance to carefully consider dosing regimens in in vitro studies as relying on single dose exposure alone may not fully capture the toxicological profiles of compounds. Consequently, this could lead to an underestimation of potential risks and safety limits. The increased sensitivity of RPTEC/TERT1 cells to brequinar with repeated exposure may be attributed to drug accumulation. Pharmacokinetic studies showed that repeated administration of brequinar, daily for five consecutive days, led to significant increases in both the area under the plasma drug concentration-time curve (AUC) and the half-life beta on day 5 compared to day 1 (Arteaga et al., 1989; de Forni et al., 1993). Another pharmacokinetic study using a similar dosing schedule suggested that this increase in AUC might be explained by a reduction in Vmax on day 5 versus day 1, according to their Michaelis-Menten model of elimination kinetics (Noe et al., 1990). These observations suggest that repeated exposure might lead to accumulation of brequinar, likely due to a reduced efficiency in its elimination process. In fact, pharmacokinetic data showed that renal clearance of brequinar was minimal (Schwartsmann et al., 1989). In addition, limited metabolism of brequinar in RPTEC/TERT1 cells could lead to increased accumulation with repeated dosing. Hence, limited metabolism and reduced elimination efficiency may result in elevated intracellular drug concentrations over time which might explain the increased toxicity in RPTEC/TERT1 cells with repeated dosing. A similar phenomenon has been described for the lipophilic compound cyclosporine A in RPTEC/TERT1 cells, where daily repeated exposure to 15 μM resulted in an intracellular accumulation to approximately 7600 μM on day 7, likely due to the saturation of the efflux transporter P-glycoprotein (*ABCB1*) (Wilmes et al., 2013). Repeated dose toxicity assessments may not necessarily increase toxicity to all compounds. For example, Secker et al. demonstrated that repeated exposure (every 48 h for a treatment period of 14 days) of RPTEC/TERT1 cells to cisplatin, gentamicin, and zoledronate decreased cell viability at lower concentrations compared to a single 24-h exposure, whereas tacrolimus decreased cell viability at similar concentrations regardless of the treatment regimen (Secker et al., 2019). Daily repeated treatment of RPTEC/TERT1 cells for 14 days with cisplatin at subcytotoxic concentrations of 0.5 and 2 μM did, however, not lead to additional significant transcriptomic changes on day 14 compared to day 1 (Wilmes et al., 2015). It should be noted that repeated exposure to a toxin may lead to a dynamic interplay between cellular damage and repair responses over time, reflecting cellular adaptation to the continued exposure.

5. Conclusions

In conclusion, our study revealed that PHH and RPTEC/TERT1 cells exhibit different sensitivities to brequinar. PHH demonstrated a lower sensitivity to brequinar, as treatment with 30 μM for 24 h did not induce any significantly DEGs, whereas more than 1000 DEGs were changed in RPTEC/TERT1 cells at this concentration. Treatment with 100 μM brequinar resulted in a notable upregulation of several phase I and II drug-metabolising enzymes after a single 24-h exposure in PHH, alongside modest activation of the UPR and Nrf2 pathways. RPTEC/TERT1 cells strongly induced the UPR, Nrf2, p53, and inflammatory responses and higher fold changes of genes were observed in response to 100 μM treatment. Additionally, repeated exposure of brequinar in RPTEC/TERT1 cells showed a strong activation of these stress response pathways at much lower concentrations (300 nM), whereas the same concentrations had little or no effect in 24-h bolus treatment regimes. Therefore, repeated exposure to a compound at lower concentrations

may provide more relevant insights into gene expression and pathways induction compared to acute exposure alone. Our findings also revealed that brequinar could adversely affect the mitochondrial function of RPTEC/TERT1 cells, as evident from the decreased basal and maximal respiration rates after a single exposure as well as the downregulation of various mitochondrial genes. Overall, our study sheds light on the cellular mechanisms in response to brequinar exposure in PHH and RPTEC/TERT1 in vitro cell models. Furthermore, our study demonstrates the importance of repeated dose toxicity assessments for certain chemicals, as single dose exposure at a lower concentration may not reveal their full impact.

CRediT authorship contribution statement

Tamara Meijer: Data curation, Formal analysis, Writing – original draft, Writing – review & editing, Methodology. **Bas ter Braak:** Data curation, Formal analysis, Writing – review & editing, Methodology. **Liesanne Loonstra-Wolters:** Data curation, Formal analysis, Methodology. **Steven J. Kunnen:** Formal analysis, Writing – review & editing. **Barira Islam:** Writing – review & editing. **Ilinca Suciu:** Writing – review & editing. **Iain Gardner:** Writing – review & editing, Methodology. **Oliver Hatley:** Writing – review & editing. **Richard Currie:** Writing – review & editing, Conceptualization. **Barry Hardy:** Formal analysis, Writing – review & editing, Conceptualization. **Marcel Leist:** Writing – review & editing, Conceptualization, Methodology. **Bob van de Water:** Writing – review & editing, Conceptualization, Methodology. **Paul Jennings:** Writing – review & editing, Conceptualization, Methodology. **Anja Wilmes:** Data curation, Formal analysis, Writing – original draft, Writing – review & editing, Conceptualization, Methodology.

Declaration of competing interest

The authors declare the following financial interests/personal relationships which may be considered as potential competing interests: Anja Wilmes reports financial support was provided by European Commission. Anja Wilmes reports financial support was provided by Syngenta Crop Protection AG. If there are other authors, they declare that they have no known competing financial interests or personal relationships that could have appeared to influence the work reported in this paper.

Acknowledgements

This work has received funding from Syngenta and from the European Union's Horizon 2020 research and innovation programme under grant agreement No 681002 (EU-ToxRisk) and grant agreement No 964537 (RISK-HUNT*3R*).

Appendix A. Supplementary data

Supplementary data to this article can be found online at https://doi.org/10.1016/j.tiv.2025.106010.

Data availability

Data are available on reasonable request from the authors.

References

Adcock, R.S., Chu, Y.-K., Golden, J.E., Chung, D.-H., 2017. Evaluation of anti-Zika virus activities of broad-spectrum antivirals and NIH clinical collection compounds using a cell-based, high-throughput screen assay. Antivir. Res. 138, 47–56. https://doi.org/10.1016/j.antiviral.2016.11.018.

Arteaga, C.L., Brown, T.D., Kuhn, J.G., Shen, H.S., O'Rourke, T.J., Beougher, K., Brentzel, H.J., Von Hoff, D.D., Weiss, G.R., 1989. Phase I clinical and pharmacokinetic trial of Brequinar sodium (DuP 785; NSC 368390). Cancer Res. 49, 4648–4653.

Aschauer, L., Gruber, L.N., Pfaller, W., Limonciel, A., Athersuch, T.J., Cavill, R., Khan, A., Gstraunthaler, G., Grillari, J., Grillari, R., Hewitt, P., Leonard, M.O., Wilmes, A., Jennings, P., 2013. Delineation of the key aspects in the regulation of epithelial monolayer formation. Mol. Cell. Biol. 33, 2535–2550. https://doi.org/10.1128/MCB.01435-12.

Aschauer, L., Limonciel, A., Wilmes, A., Stanzel, S., Kopp-Schneider, A., Hewitt, P., Lukas, A., Leonard, M.O., Pfaller, W., Jennings, P., 2015. Application of RPTEC/TERT1 cells for investigation of repeat dose nephrotoxicity: a transcriptomic study. Toxicol. in Vitro 30, 106–116. https://doi.org/10.1016/j.tiv.2014.10.005.

Banerjee, R., Purhonen, J., Kallijärvi, J., 2022. The mitochondrial coenzyme Q junction and complex III: biochemistry and pathophysiology. FEBS J. 289, 6936–6958. https://doi.org/10.1111/febs.16164.

Baumgartner, R., Walloschek, M., Kralik, M., Gotschlich, A., Tasler, S., Mies, J., Leban, J., 2006. Dual binding mode of a novel series of DHODH inhibitors. J. Med. Chem. 49, 1239–1247. https://doi.org/10.1021/jm0506975.

Bell, C.C., Hendriks, D.F.G., Moro, S.M.L., Ellis, E., Walsh, J., Renblom, A., Fredriksson Puigvert, L., Dankers, A.C.A., Jacobs, F., Snoeys, J., Sison-Young, R.L., Jenkins, R.E., Nordling, Å., Mkrtchian, S., Park, B.K., Kitteringham, N.R., Goldring, C.E.P., Lauschke, V.M., Ingelman-Sundberg, M., 2016. Characterization of primary human hepatocyte spheroids as a model system for drug-induced liver injury, liver function and disease. Sci. Rep. 6, 25187. https://doi.org/10.1038/srep25187.

Bhattacharya, S., Zhang, Q., Carmichael, P.L., Boekelheide, K., Andersen, M.E., 2011. Toxicity testing in the 21st century: defining new risk assessment approaches based on perturbation of intracellular toxicity pathways. PLoS One 6, e20887. https://doi.org/10.1371/journal.pone.0020887.

Bork, E., Vest, S., Hansen, H.H., 1989. A phase I clinical and pharmacokinetic study of brequinar sodium, DUP 785 (NSC 368390), using a weekly and a biweekly schedule. Eur. J. Cancer Clin. Oncol. 25, 1403–1411. https://doi.org/10.1016/0277-5379(89)90097-7.

Capinha, L., Zhang, Y., Holzer, A.-K., Ückert, A.-K., Zana, M., Carta, G., Murphy, C., Baldovini, J., Mazidi, Z., Grillari, J., Dinnyes, A., van de Water, B., Leist, M., Commandeur, J.N.M., Jennings, P., 2023. Transcriptomic-based evaluation of trichloroethylene glutathione and cysteine conjugates demonstrate phenotype-dependent stress responses in a panel of human in vitro models. Arch. Toxicol. 97, 523–545. https://doi.org/10.1007/s00204-022-03436-6.

Carta, G., van der Stel, W., Scuric, E.W.J., Capinha, L., Delp, J., Bennekou, S.H., Forsby, A., Walker, P., Leist, M., van de Water, B., Jennings, P., 2023. Transcriptional landscape of mitochondrial electron transport chain inhibition in renal cells. Cell Biol. Toxicol. 39, 3031–3059. https://doi.org/10.1007/s10565-023-09816-7.

Chen, J.-J., Jones, M.E., 1976. The cellular location of dihydroorotate dehydrogenase: relation to de novo biosynthesis of pyrimidines. Arch. Biochem. Biophys. 176, 82–90. https://doi.org/10.1016/0003-9861(76)90143-0.

Chen, S.-F., Ruben, R.L., Dexter, D.L., 1986. Mechanism of action of the novel anticancer agent 6-Fluoro-2-(2′-fluoro-1,1′-biphenyl-4-yl)-3-methyl-4-quinolinecarboxylic acid sodium salt (NSC 368390): inhibition of de novo pyrimidine nucleotide biosynthesis. Cancer Res. 46, 5014–5019.

Cody, R., Stewart, D., DeForni, M., Moore, M., Dallaire, B., Azarnia, N., Gyves, J., 1993. Multicenter phase II study of Brequinar sodium in patients with advanced breast Cancer. Am. J. Clin. Oncol. 16, 526–528. https://doi.org/10.1097/00000421-199312000-00014.

Cosenza, C.A., Cramer, D.V., Eiras-Hreha, G., Cajulis, E., Wang, H.K., Makowka, L., 1993. The synergism of brequinar sodium and cyclosporine used in combination to prevent cardiac allograft rejection in the rat. Transplantation 56, 667–671. https://doi.org/10.1097/00007890-199309000-00032.

de Forni, M., Armand, J.-P., Fontana, X., Recondo, G., Domenge, C., Carde, P., Chabot, G. G., Gouyette, A., Barbu, M., 1993. Phase I and pharmacokinetic study of brequinar (DUP 785; NSC 368390) in cancer patients. Eur. J. Cancer 29, 983–988. https://doi.org/10.1016/S0959-8049(05)80206-0.

Demarest, J.F., Kienle, M., Boytz, R., Ayres, M., Kim, E.J., Patten, J.J., Chung, D., Gandhi, V., Davey, R.A., Sykes, D.B., Shohdy, N., Pottage, J.C., Kumar, V.S., 2022. Brequinar and dipyridamole in combination exhibits synergistic antiviral activity against SARS-CoV-2 in vitro: rationale for a host-acting antiviral treatment strategy for COVID-19. Antivir. Res. 206, 105403. https://doi.org/10.1016/j.antiviral.2022.105403.

Devarajan, P., 2008. Neutrophil gelatinase-associated lipocalin (NGAL): a new marker of kidney disease. Scand. J. Clin. Lab. Invest. 68, 89–94. https://doi.org/10.1080/00365510802150158.

Dexter, D.L., Hesson, D.P., Ardecky, R.J., Rao, G.V., Tippett, D.L., Dusak, B.A., Paull, K. D., Plowman, J., DeLarco, B.M., Narayanan, V.L., 1985. Activity of a novel 4-quinolinecarboxylic acid, NSC 368390 [6-fluoro-2-(2′-fluoro-1,1′-biphenyl-4-yl)-3-methyl-4-quinolinecarb oxylic acid sodium salt], against experimental tumors. Cancer Res. 45, 5563–5568.

di Masi, A., De Marinis, E., Ascenzi, P., Marino, M., 2009. Nuclear receptors CAR and PXR: molecular, functional, and biomedical aspects. Mol. Asp. Med. 30, 297–343. https://doi.org/10.1016/j.mam.2009.04.002.

Dodion, P.F., Wagener, T., Stoter, G., Drozd, A., Lev, L.M., Skovsgaard, T., Renard, J., Cavalli, F., 1990. Phase II trial with Brequinar (DUP-785, NSC 368390) in patients with metastatic colorectal cancer: a study of the early clinical trials group of the EORTC. Ann. Oncol. 1, 79–80. https://doi.org/10.1093/oxfordjournals.annonc.a057680.

Fernandes, H.J.R., Patikas, N., Foskolou, S., Field, S.F., Park, J.-E., Byrne, M.L., Bassett, A.R., Metzakopian, E., 2020. Single-cell transcriptomics of Parkinson's disease human in vitro models reveals dopamine neuron-specific stress responses. Cell Rep. 33, 108263. https://doi.org/10.1016/j.celrep.2020.108263.

Fischer, I., Milton, C., Wallace, H., 2020. Toxicity testing is evolving. Toxicol. Res. (Camb.) 9, 67–80. https://doi.org/10.1093/toxres/tfaa011.
Fontecha-Barriuso, M., Martín-Sánchez, D., Martinez-Moreno, J.M., Carrasco, S., Ruiz-Andrés, O., Monsalve, M., Sanchez-Ramos, C., Gómez, M.J., Ruiz-Ortega, M., Sánchez-Niño, M.D., Cannata-Ortiz, P., Cabello, R., Gonzalez-Enguita, C., Ortiz, A., Sanz, A.B., 2019. PGC-1α deficiency causes spontaneous kidney inflammation and increases the severity of nephrotoxic AKI. J. Pathol. 249, 65–78. https://doi.org/10.1002/path.5282.
Fontecha-Barriuso, M., Martin-Sanchez, D., Martinez-Moreno, J., Monsalve, M., Ramos, A., Sanchez-Niño, M., Ruiz-Ortega, M., Ortiz, A., Sanz, A., 2020. The role of PGC-1α and mitochondrial biogenesis in kidney diseases. Biomolecules 10, 347. https://doi.org/10.3390/biom10020347.
Garcia, I., Jones, E., Ramos, M., Innis-Whitehouse, W., Gilkerson, R., 2017. The little big genome: the organization of mitochondrial DNA. Front. Biosci. 22, 710–721. https://doi.org/10.2741/4511.
Gu, Z., 2022. Complex heatmap visualization. iMeta 1, e43. https://doi.org/10.1002/imt2.43.
Gu, Z., Gu, L., Eils, R., Schlesner, M., Brors, B., 2014. Circlize implements and enhances circular visualization in R. Bioinformatics 30, 2811–2812. https://doi.org/10.1093/bioinformatics/btu393.
Herwig, R., Hardt, C., Lienhard, M., Kamburov, A., 2016. Analyzing and interpreting genome data at the network level with ConsensusPathDB. Nat. Protoc. 11, 1889–1907. https://doi.org/10.1038/nprot.2016.117.
Heslop, J.A., Rowe, C., Walsh, J., Sison-Young, R., Jenkins, R., Kamalian, L., Kia, R., Hay, D., Jones, R.P., Malik, H.Z., Fenwick, S., Chadwick, A.E., Mills, J., Kitteringham, N.R., Goldring, C.E.P., Kevin Park, B., 2017. Mechanistic evaluation of primary human hepatocyte culture using global proteomic analysis reveals a selective dedifferentiation profile. Arch. Toxicol. 91, 439–452. https://doi.org/10.1007/s00204-016-1694-y.
Jennings, P., Limonciel, A., Felice, L., Leonard, M.O., 2013. An overview of transcriptional regulation in response to toxicological insult. Arch. Toxicol. 87, 49–72. https://doi.org/10.1007/s00204-012-0919-y.
Jennings, P., Carta, G., Singh, P., da Costa Pereira, D., Feher, A., Dinnyes, A., Exner, T.E., Wilmes, A., 2023. Capturing time-dependent activation of genes and stress-response pathways using transcriptomics in iPSC-derived renal proximal tubule cells. Cell Biol. Toxicol. 39, 1773–1793. https://doi.org/10.1007/s10565-022-09783-5.
Jones, S.W., Penman, S.L., French, N.S., Park, B.K., Chadwick, A.E., 2021. Investigating dihydroorotate dehydrogenase inhibitor mediated mitochondrial dysfunction in hepatic in vitro models. Toxicol. in Vitro 72, 105096. https://doi.org/10.1016/j.tiv.2021.105096.
Joshi, A.S., King, S.P., Zajac, B.A., Makowka, L., Sher, L.S., Kahan, B.D., Menkis, A.H., Stiller, C.R., Schaefle, B., Kornhauser, D.M., 1997. Phase I safety and pharmacokinetic studies of Brequinar sodium after single ascending Oral doses in stable renal, hepatic, and cardiac allograft recipients. J. Clin. Pharmacol. 37, 1121–1128. https://doi.org/10.1002/j.1552-4604.1997.tb04296.x.
Kamburov, A., Herwig, R., 2022. ConsensusPathDB 2022: molecular interactions update as a resource for network biology. Nucleic Acids Res. 50, D587–D595. https://doi.org/10.1093/nar/gkab1128.
Kamburov, A., Pentchev, K., Galicka, H., Wierling, C., Lehrach, H., Herwig, R., 2011. ConsensusPathDB: toward a more complete picture of cell biology. Nucleic Acids Res. 39, D712–D717. https://doi.org/10.1093/nar/gkq1156.
Khutornenko, A.A., Roudko, V.V., Chernyak, B.V., Vartapetian, A.B., Chumakov, P.M., Evstafieva, A.G., 2010. Pyrimidine biosynthesis links mitochondrial respiration to the p53 pathway. Proc. Natl. Acad. Sci. 107, 12828–12833. https://doi.org/10.1073/pnas.0910885107.
Krauskopf, J., Eggermont, K., Madeiro Da Costa, R.F., Bohler, S., Hauser, D., Caiment, F., de Kok, T.M., Verfaillie, C., Kleinjans, J.C., 2022. Transcriptomics analysis of human iPSC-derived dopaminergic neurons reveals a novel model for sporadic Parkinson's disease. Mol. Psychiatry 27, 4355–4367. https://doi.org/10.1038/s41380-022-01663-y.
Ladds, M.J.G.W., van Leeuwen, I.M.M., Drummond, C.J., Chu, S., Healy, A.R., Popova, G., Pastor Fernández, A., Mollick, T., Darekar, S., Sedimbi, S.K., Nekulova, M., Sachweh, M.C.C., Campbell, J., Higgins, M., Tuck, C., Popa, M., Safont, M.M., Gelebart, P., Fandalyuk, Z., Thompson, A.M., Svensson, R., Gustavsson, A.-L., Johansson, L., Färnegårdh, K., Yngve, U., Saleh, A., Haraldsson, M., D'Hollander, A.C.A., Franco, M., Zhao, Y., Håkansson, M., Walse, B., Larsson, K., Peat, E.M., Pelechano, V., Lunec, J., Vojtesek, B., Carmena, M., Earnshaw, W.C., McCarthy, A.R., Westwood, N.J., Arsenian-Henriksson, M., Lane, D. P., Bhatia, R., McCormack, E., Laín, S., 2018. A DHODH inhibitor increases p53 synthesis and enhances tumor cell killing by p53 degradation blockage. Nat. Commun. 9, 1107. https://doi.org/10.1038/s41467-018-03441-3.
LaGory, E.L., Wu, C., Taniguchi, C.M., Ding, C.-K.C., Chi, J.-T., von Eyben, R., Scott, D.A., Richardson, A.D., Giaccia, A.J., 2015. Suppression of PGC-1α is critical for reprogramming oxidative metabolism in renal cell carcinoma. Cell Rep. 12, 116–127. https://doi.org/10.1016/j.celrep.2015.06.006.
Lim, Y.-P., Huang, J., 2008. Interplay of Pregnane X receptor with other nuclear receptors on gene regulation. Drug Metab. Pharmacokinet. 23, 14–21. https://doi.org/10.2133/dmpk.23.14.
Limonciel, A., Aschauer, L., Wilmes, A., Prajczer, S., Leonard, M.O., Pfaller, W., Jennings, P., 2011. Lactate is an ideal non-invasive marker for evaluating temporal alterations in cell stress and toxicity in repeat dose testing regimes. Toxicol. in Vitro 25, 1855–1862. https://doi.org/10.1016/j.tiv.2011.05.018.
Limonciel, A., Wilmes, A., Aschauer, L., Radford, R., Bloch, K.M., McMorrow, T., Pfaller, W., van Delft, J.H., Slattery, C., Ryan, M.P., Lock, E.A., Jennings, P., 2012. Oxidative stress induced by potassium bromate exposure results in altered tight junction protein expression in renal proximal tubule cells. Arch. Toxicol. 86, 1741–1751. https://doi.org/10.1007/s00204-012-0897-0.
Limonciel, A., Ates, G., Carta, G., Wilmes, A., Watzele, M., Shepard, P.J., VanSteenhouse, H.C., Seligmann, B., Yeakley, J.M., van de Water, B., Vinken, M., Jennings, P., 2018a. Comparison of base-line and chemical-induced transcriptomic responses in HepaRG and RPTEC/TERT1 cells using TempO-Seq. Arch. Toxicol. 92, 2517–2531. https://doi.org/10.1007/s00204-018-2256-2.
Limonciel, A., van Breda, S.G., Jiang, X., Tredwell, G.D., Wilmes, A., Aschauer, L., Siskos, A.P., Sachinidis, A., Keun, H.C., Kopp-Schneider, A., de Kok, T.M., Kleinjans, J.C.S., Jennings, P., 2018b. Persistence of Epigenomic effects after recovery from repeated treatment with two Nephrocarcinogens. Front. Genet. 9, 558. https://doi.org/10.3389/fgene.2018.00558.
Linke, S.P., Clarkin, K.C., Di Leonardo, A., Tsou, A., Wahl, G.M., 1996. A reversible, p53-dependent G0/G1 cell cycle arrest induced by ribonucleotide depletion in the absence of detectable DNA damage. Genes Dev. 10, 934–947. https://doi.org/10.1101/gad.10.8.934.
Liu, S., Neidhardt, E.A., Grossman, T.H., Ocain, T., Clardy, J., 2000. Structures of human dihydroorotate dehydrogenase in complex with antiproliferative agents. Structure 8, 25–33. https://doi.org/10.1016/S0969-2126(00)00077-0.
Liu, T., Zhang, L., Joo, D., Sun, S.-C., 2017. NF-κB signaling in inflammation. Signal Transduct. Target. Ther. 2, 17023. https://doi.org/10.1038/sigtrans.2017.23.
Love, M.I., Huber, W., Anders, S., 2014. Moderated estimation of fold change and dispersion for RNA-seq data with DESeq2. Genome Biol. 15, 550. https://doi.org/10.1186/s13059-014-0550-8.
Madak, J.T., Bankhead, A., Cuthbertson, C.R., Showalter, H.D., Neamati, N., 2019. Revisiting the role of dihydroorotate dehydrogenase as a therapeutic target for cancer. Pharmacol. Ther. 195, 111–131. https://doi.org/10.1016/j.pharmthera.2018.10.012.
Makowka, L., Sher, L.S., Cramer, D.V., 1993. The development of Brequinar as an immunosuppressive drug for transplantation. Immunol. Rev. 136, 51–70. https://doi.org/10.1111/j.1600-065X.1993.tb00654.x.
Maroun, J., Ruckdeschel, J., Natale, R., Morgan, R., Dallaire, B., Sisk, R., Gyves, J., 1993. Multicenter phase II study of brequinar sodium in patients with advanced lung cancer. Cancer Chemother. Pharmacol. 32, 64–66. https://doi.org/10.1007/BF00685878.
Moore, M., Maroun, J., Robert, F., Natale, R., Neidhart, J., Dallaire, B., Sisk, R., Gyves, J., 1993. Multicenter phase II study of brequinar sodium in patients with advanced gastrointestinal cancer. Investig. New Drugs 11, 61–65. https://doi.org/10.1007/BF00873913.
Murphy, C., Jennings, P., Wilmes, A., 2024. Transcriptomic profile of human iPSC-derived podocyte-like cells exposed to a panel of xenobiotics. Toxicol. in Vitro 97, 105804. https://doi.org/10.1016/j.tiv.2024.105804.
Natale, R., Wheeler, R., Moore, M., Dallaire, B., Lynch, W., Carlson, R., Grillo-Lopez, A., Gyves, J., 1992. Short report: multicenter phase II trial of brequinar sodium in patients with advanced melanoma. Ann. Oncol. 3, 659–660. https://doi.org/10.1093/oxfordjournals.annonc.a058298.
Niemeijer, M., Więcek, W., Fu, S., Huppelschoten, S., Bouwman, P., Baze, A., Parmentier, C., Richert, L., Paules, R.S., Bois, F.Y., van de Water, B., 2024. Mapping Interindividual variability of Toxicodynamics using high-throughput transcriptomics and primary human hepatocytes from fifty donors. Environ. Health Perspect. 132, 37005. https://doi.org/10.1289/EHP11891.
Noe, D.A., Rowinsky, E.K., Shen, H.-S.L., Clarke, B.V., Grochow, L.B., McGuire, W.B., Hantel, A., Adams, D.B., Abeloff, M.D., Ettinger, D.S., Donehower, R.C., 1990. Phase I and pharmacokinetic study of Brequinar sodium (NSC 368390). Cancer Res. 50, 4595–4599.
Nunes, C., Singh, P., Mazidi, Z., Murphy, C., Bourguignon, A., Wellens, S., Chandrasekaran, V., Ghosh, S., Zana, M., Pamies, D., Thomas, A., Verfaillie, C., Culot, M., Dinnyes, A., Hardy, B., Wilmes, A., Jennings, P., Grillari, R., Grillari, J., Zurich, M.-G., Exner, T., 2022. An in vitro strategy using multiple human induced pluripotent stem cell-derived models to assess the toxicity of chemicals: a case study on paraquat. Toxicol. in Vitro 81, 105333. https://doi.org/10.1016/j.tiv.2022.105333.
Peters, G.J., Sharma, S.L., Laurensse, E., Pinedo, H.M., 1987. Inhibition of pyrimidine de novo synthesis by DUP-785 (NSC 368390). Investig. New Drugs 5, 235–244. https://doi.org/10.1007/BF00175293.
Peters, G.J., Schwartsmann, G., Nadal, J.C., Laurensse, E.J., van Groeningen, C.J., van der Vijgh, W.J., Pinedo, H.M., 1990. In vivo inhibition of the pyrimidine de novo enzyme dihydroorotic acid dehydrogenase by brequinar sodium (DUP-785; NSC 368390) in mice and patients. Cancer Res. 50, 4644–4649.
Qing, M., Zou, G., Wang, Q.-Y., Xu, H.Y., Dong, H., Yuan, Z., Shi, P.-Y., 2010. Characterization of dengue virus resistance to Brequinar in cell culture. Antimicrob. Agents Chemother. 54, 3686–3695. https://doi.org/10.1128/AAC.00561-10.
Rath, S., Sharma, R., Gupta, R., Ast, T., Chan, C., Durham, T.J., Goodman, R.P., Grabarek, Z., Haas, M.E., Hung, W.H.W., Joshi, P.R., Jourdain, A.A., Kim, S.H., Kotrys, A.V., Lam, S.S., McCoy, J.G., Meisel, J.D., Miranda, M., Panda, A., Patgiri, A., Rogers, R., Sadre, S., Shah, H., Skinner, O.S., To, T.-L., Walker, M.A., Wang, H., Ward, P.S., Wengrod, J., Yuan, C.-C., Calvo, S.E., Mootha, V.K., 2021. MitoCarta3.0: an updated mitochondrial proteome now with sub-organelle localization and pathway annotations. Nucleic Acids Res. 49, D1541–D1547. https://doi.org/10.1093/nar/gkaa1011.
Rawls, J., Knecht, W., Diekert, K., Lill, R., Löffler, M., 2000. Requirements for the mitochondrial import and localization of dihydroorotate dehydrogenase. Eur. J. Biochem. 267, 2079–2087. https://doi.org/10.1046/j.1432-1327.2000.01213.x.
Rosales, M.A.B., Shu, D.Y., Iacovelli, J., Saint-Geniez, M., 2019. Loss of PGC-1α in RPE induces mesenchymal transition and promotes retinal degeneration. Life Sci. Alliance 2, e201800212. https://doi.org/10.26508/lsa.201800212.

Schmeisser, S., Miccoli, A., von Bergen, M., Berggren, E., Braeuning, A., Busch, W., Desaintes, C., Gourmelon, A., Grafström, R., Harrill, J., Hartung, T., Herzler, M., Kass, G.E.N., Kleinstreuer, N., Leist, M., Luijten, M., Marx-Stoelting, P., Poetz, O., van Ravenzwaay, B., Roggeband, R., Rogiers, V., Roth, A., Sanders, P., Thomas, R.S., Marie Vinggaard, A., Vinken, M., van de Water, B., Luch, A., Tralau, T., 2023. New approach methodologies in human regulatory toxicology – not if, but how and when! Environ. Int. 178, 108082. https://doi.org/10.1016/j.envint.2023.108082.

Schwartsmann, G., Peters, G.J., Laurensse, E., de Waal, F.C., Loonen, A.H., Leyva, A., Pinedo, H.M., 1988. DUP 785 (NSC 368390): schedule-dependency of growth-inhibitory and antipyrimidine effects. Biochem. Pharmacol. 37, 3257–3266. https://doi.org/10.1016/0006-2952(88)90636-3.

Schwartsmann, G., van der Vijgh, W.J.F., van Hennik, M.B., Klein, I., Vermorken, J.B., Dodion, P., ten Bokkel Huinink, W.W., Joggi, G., Gall, H., Crespeigne, N., Simonetti, G., Winograd, B., Pinedo, H.M., 1989. Pharmacokinetics of Brequinar sodium (NSC 368390) in patients with solid tumors during a phase I study. Eur. J. Cancer Clin. Oncol. 25, 1675–1681. https://doi.org/10.1016/0277-5379(89)90334-9.

Secker, P.F., Schlichenmaier, N., Beilmann, M., Deschl, U., Dietrich, D.R., 2019. Functional transepithelial transport measurements to detect nephrotoxicity in vitro using the RPTEC/TERT1 cell line. Arch. Toxicol. 93, 1965–1978. https://doi.org/10.1007/s00204-019-02469-8.

Sewell, F., Alexander-White, C., Brescia, S., Currie, R.A., Roberts, R., Roper, C., Vickers, C., Westmoreland, C., Kimber, I., 2024. New approach methodologies (NAMs): identifying and overcoming hurdles to accelerated adoption. Toxicol. Res. (Camb.) 13, tfae044. https://doi.org/10.1093/toxres/tfae044.

Stallons, L.J., Whitaker, R.M., Schnellmann, R.G., 2014. Suppressed mitochondrial biogenesis in folic acid-induced acute kidney injury and early fibrosis. Toxicol. Lett. 224, 326–332. https://doi.org/10.1016/j.toxlet.2013.11.014.

Sykes, D.B., 2018. The emergence of dihydroorotate dehydrogenase (DHODH) as a therapeutic target in acute myeloid leukemia. Expert Opin. Ther. Targets 22, 893–898. https://doi.org/10.1080/14728222.2018.1536748.

Sykes, D.B., Kfoury, Y.S., Mercier, F.E., Wawer, M.J., Law, J.M., Haynes, M.K., Lewis, T. A., Schajnovitz, A., Jain, E., Lee, D., Meyer, H., Pierce, K.A., Tolliday, N.J., Waller, A., Ferrara, S.J., Eheim, A.L., Stoeckigt, D., Maxcy, K.L., Cobert, J.M., Bachand, J., Szekely, B.A., Mukherjee, S., Sklar, L.A., Kotz, J.D., Clish, C.B., Sadreyev, R.I., Clemons, P.A., Janzer, A., Schreiber, S.L., Scadden, D.T., 2016. Inhibition of dihydroorotate dehydrogenase overcomes differentiation blockade in acute myeloid leukemia. Cell 167, 171–186.e15. https://doi.org/10.1016/j.cell.2016.08.057.

Takakura, Y., Machida, M., Terada, N., Katsumi, Y., Kawamura, S., Horie, K., Miyauchi, M., Ishikawa, T., Akiyama, N., Seki, T., Miyao, T., Hayama, M., Endo, R., Ishii, H., Maruyama, Y., Hagiwara, N., Kobayashi, T.J., Yamaguchi, Naoto, Takano, H., Akiyama, T., Yamaguchi, Noritaka, 2024. Mitochondrial protein C15ORF48 is a stress-independent inducer of autophagy that regulates oxidative stress and autoimmunity. Nat. Commun. 15, 953. https://doi.org/10.1038/s41467-024-45206-1.

ter Braak, B., Niemeijer, M., Boon, R., Parmentier, C., Baze, A., Richert, L., Huppelschoten, S., Wink, S., Verfaillie, C., van de Water, B., 2021. Systematic transcriptome-based comparison of cellular adaptive stress response activation networks in hepatic stem cell-derived progeny and primary human hepatocytes. Toxicol. in Vitro 73, 105107. https://doi.org/10.1016/j.tiv.2021.105107.

Urba, S., Doroshow, J., Cripps, C., Robert, F., Velez-Garcia, E., Dallaire, B., Adams, D., Carlson, R., Grillo-Lopez, A., Gyves, J., 1992. Multicenter phase II trial of brequinar sodium in patients with advanced squamous-cell carcinoma of the head and neck. Cancer Chemother. Pharmacol. 31, 167–169. https://doi.org/10.1007/BF00685106.

Utkarsh, D., Loretz, C., Li, A.P., 2016. In vitro evaluation of hepatotoxic drugs in human hepatocytes from multiple donors: identification of P450 activity as a potential risk factor for drug-induced liver injuries. Chem. Biol. Interact. 255, 12–22. https://doi.org/10.1016/j.cbi.2015.12.013.

van der Stel, W., Carta, G., Eakins, J., Darici, S., Delp, J., Forsby, A., Bennekou, S.H., Gardner, I., Leist, M., Danen, E.H.J., Walker, P., van de Water, B., Jennings, P., 2020. Multiparametric assessment of mitochondrial respiratory inhibition in HepG2 and RPTEC/TERT1 cells using a panel of mitochondrial targeting agrochemicals. Arch. Toxicol. 94, 2707–2729. https://doi.org/10.1007/s00204-020-02792-5.

Wang, Y.-M., Ong, S.S., Chai, S.C., Chen, T., 2012. Role of CAR and PXR in xenobiotic sensing and metabolism. Expert Opin. Drug Metab. Toxicol. 8, 803–817. https://doi.org/10.1517/17425255.2012.685237.

Wickham, H., Averick, M., Bryan, J., Chang, W., McGowan, L., François, R., Grolemund, G., Hayes, A., Henry, L., Hester, J., Kuhn, M., Pedersen, T., Miller, E., Bache, S., Müller, K., Ooms, J., Robinson, D., Seidel, D., Spinu, V., Takahashi, K., Vaughan, D., Wilke, C., Woo, K., Yutani, H., 2019. Welcome to the Tidyverse. J. Open Source Softw. 4, 1686. https://doi.org/10.21105/joss.01686.

Wieser, M., Stadler, G., Jennings, P., Streubel, B., Pfaller, W., Ambros, P., Riedl, C., Katinger, H., Grillari, J., Grillari-Voglauer, R., 2008. hTERT alone immortalizes epithelial cells of renal proximal tubules without changing their functional characteristics. Am. J. Physiol. Physiol. 295, F1365–F1375. https://doi.org/10.1152/ajprenal.90405.2008.

Wilmes, A., Limonciel, A., Aschauer, L., Moenks, K., Bielow, C., Leonard, M.O., Hamon, J., Carpi, D., Ruzek, S., Handler, A., Schmal, O., Herrgen, K., Bellwon, P., Burek, C., Truisi, G.L., Hewitt, P., Di Consiglio, E., Testai, E., Blaauboer, B.J., Guillou, C., Huber, C.G., Lukas, A., Pfaller, W., Mueller, S.O., Bois, F.Y., Dekant, W., Jennings, P., 2013. Application of integrated transcriptomic, proteomic and metabolomic profiling for the delineation of mechanisms of drug induced cell stress. J. Proteome 79, 180–194. https://doi.org/10.1016/j.jprot.2012.11.022.

Wilmes, A., Aschauer, L., Limonciel, A., Pfaller, W., Jennings, P., 2014. Evidence for a role of claudin 2 as a proximal tubular stress responsive paracellular water channel. Toxicol. Appl. Pharmacol. 279, 163–172. https://doi.org/10.1016/j.taap.2014.05.013.

Wilmes, A., Bielow, C., Ranninger, C., Bellwon, P., Aschauer, L., Limonciel, A., Chassaigne, H., Kristl, T., Aiche, S., Huber, C.G., Guillou, C., Hewitt, P., Leonard, M. O., Dekant, W., Bois, F., Jennings, P., 2015. Mechanism of cisplatin proximal tubule toxicity revealed by integrating transcriptomics, proteomics, metabolomics and biokinetics. Toxicol. in Vitro 30, 117–127. https://doi.org/10.1016/j.tiv.2014.10.006.

Zheng, L., Zhou, M., Guo, Z., Lu, H., Qian, L., Dai, H., Qiu, J., Yakubovskaya, E., Bogenhagen, D.F., Demple, B., Shen, B., 2008. Human DNA2 is a mitochondrial nuclease/helicase for efficient processing of DNA replication and repair intermediates. Mol. Cell 32, 325–336. https://doi.org/10.1016/j.molcel.2008.09.024.